

A new application of reduced Rayleigh equations to electromagnetic wave scattering by two-dimensional randomly rough surfaces

Antoine Soubret,^{1,2,†} Gérard Berginc,¹ and Claude Bourrely²

¹*Thomson-CSF Optronique, BP 55, 78233 Guyancourt Cedex, France.*

²*Centre de Physique Théorique, CNRS-Luminy Case 907, 13288 Marseille Cedex 9, France.*

(Dated: September 2000)

The small perturbations method has been extensively used for waves scattering by rough surfaces. The standard method developed by Rice is difficult to apply when we consider second and third order of scattered fields as a function of the surface height. Calculations can be greatly simplified with the use of reduced Rayleigh equations, because one of the unknown fields can be eliminated. We derive a new set of four reduced equations for the scattering amplitudes, which are applied to the cases of a rough conducting surface, and to a slab where one of the boundary is a rough surface. As in the one-dimensional case, numerical simulations show the appearance of enhanced backscattering for these structures.

I. INTRODUCTION

The scattering of electromagnetic waves from a rough surface has been studied in different domains such as radio-physics, geophysical remote sensing, ocean acoustics, and surface optics.^{1,2,3,4,5,6,7,8,9,10,11} One of the earlier theory used, is the small perturbations method (SPM) originally developed by Rice,¹² this theory still remains of interest^{11,13,14} because perturbative terms of order higher than one can produce enhanced backscattering, or improve predictions accuracy in an emission model. Although, the Rice method can be used in principle to determine all orders in the perturbative development, very few works use terms of order higher than one for a two-dimensional surface due to the calculations complexity. The second order has been written in a compact form by Voronovich¹⁵ in his work on small-slope approximation, and only recently the third order has been presented.¹³ However, there exists a different way to obtain (SPM) which dates back from the work of Brown *et al.*¹⁶ Using both the Rayleigh hypothesis and the extinction theorem, they have obtained an integral equation, called the reduced Rayleigh equation, which only involves the incident and the scattered field alone. In their method the field transmitted through the surface has been eliminated in such a way that the scattered field becomes a function of the incident field only. This reduced equation has been extensively used by Maradudin *et al.* to study localization effects by a conducting surface,^{17,18,19} coherent effects in reflection factor,²⁰ scattering by one-dimensional²¹ and two-dimensional conducting surface.²² It has to be noticed that the third order perturbation term was already explicited in the work of Ref. 22.

In recent years, similar studies have been done in the case of thin films bounded by a rough surface,^{11,23} but only in the one-dimensional case.³² In order to calculate the two-dimensional case it becomes necessary to derive an extension of the reduced Rayleigh equation for this system. In the present paper, we first study a surface where a down-going and up-going fields exist both on the upper and the bottom side of the film. We show the existence of four equations, that we also call reduced Rayleigh equation, they have the property that one of the down-going or up-going fields has been eliminated. With these equations, we rediscover the equation obtained by Brown *et al.*¹⁶ for one rough surface, and derive the corresponding ones for a slab where one of the boundary is a rough surface. Next, a perturbative development up to third order is obtained in a compact matrix form for these two systems. This third order term is mandatory if we need the expression of the cross section up to fourth order approximation. As in the one-dimensional case, the results of the incoherent cross section show a well defined peak in the retroreflection direction.

In the case of small-roughness metallic surfaces this peak was originally explained by the infinite perturbation theory,^{17,18,19} and further developments²¹ have shown that the major contribution for the enhanced backscattering peak comes from the second order term in the field perturbation. However, in the one dimensional case the enhanced backscattering for a rough surface, appears only for a (*TM*) incident wave due to the fact that plasmons polaritons only exist for this polarization. In the two dimensional case, due to the existence of cross-polarization, we will show that an incident (*TE*) wave can excite a (*TM*) plasmon mode which can transform into a (*TE*) or (*TM*) volume electromagnetic wave. Thus,

the enhanced backscattering is present independently of the polarization of the incident and scattered waves. For a rough dielectric film bounded by a conducting plane the enhanced backscattering is present for both (TE) and (TM) incident waves, even in the one-dimensional case because guided waves exist for these two polarizations. The qualitative effect of the two-dimensional surface is particularly sensitive when we study thin film, for instance, in one-dimensional case, satellite peaks^{11,23} appear on each side of the enhanced backscattering peaks, however, in the two-dimensional case, the coupling between (TE) and (TM) modes attenuates drastically these peaks.

The paper is organized as follows. In Sec. II, we derive the four new reduced Rayleigh equations. In Sec. III, we introduce the diffusion matrix, and in Sec. IV, we determine the perturbative development up to third order term in the surface height, for a rough surface alone, and for slab with a rough surface located at one of the boundaries. In Sec. V, we introduce the Mueller matrix and the definition of the statistical parameters for the rough surface. We then obtain the bistatic matrix in terms of a perturbative development. Numerical examples which show the enhanced backscattering are presented in Sec. VI. Conclusions drawn from the results of our calculations are discussed in Sec. VII.

II. DERIVATION OF THE REDUCED RAYLEIGH EQUATION

The reduced Rayleigh equation was obtained for a two-dimensional surface by Brown *et al.*¹⁶ using the extinction theorem and the Rayleigh hypothesis, it allows to calculate the scattered field from the rough surface. Now, if we want to compute the transmitted field from the rough surface, one has to introduce an other reduced Rayleigh equation derived by Greffet.²⁴ However, these two equations were established in the case where there is no up-going field inside the medium, thus they cannot be used to obtain the field scattered by a slab with a rough surface in its upper side. In fact, to generalize these equations to a slab, we have to consider all the fields shown in Fig. 1. We will prove that there exists four reduced Rayleigh equations, which involve only three of the participating fields $\mathbf{E}_0^-, \mathbf{E}_0^+, \mathbf{E}_1^-, \mathbf{E}_1^+$.

We consider that each electromagnetic waves propagates with a frequency ω , and in the following the factor $\exp(-i\omega t)$ will be omitted. We choose to work with a Cartesian coordinate system $\mathbf{r} = (\mathbf{x}, z) = (x, y, z)$, where the z axis directed upward, and we consider a boundary of the form $z = h(\mathbf{x})$. Moreover, we suppose that there exists a length L for which $h(x, y) = 0$, if $|x| > L/2$ or $|y| > L/2$, L may be arbitrary large but finite.

A Propagation equations and boundary conditions

The electric field \mathbf{E} satisfies the Helmholtz equation in the two media:

$$(\nabla^2 + \epsilon_0 K_0^2) \mathbf{E}^0(\mathbf{r}) = 0 \quad \text{for } z > h(\mathbf{x}), \quad (1)$$

$$(\nabla^2 + \epsilon_1 K_0^2) \mathbf{E}^1(\mathbf{r}) = 0 \quad \text{for } z < h(\mathbf{x}), \quad (2)$$

where $K_0 = \omega/c$. Since the system is homogeneous in the $\mathbf{x} = (x, y)$ directions, we can represent the electric field by its Fourier transform. Thus, using the Helmholtz equation, we deduce the following expression for the electric field^{8,10} in the medium 0 :

$$\mathbf{E}^0(\mathbf{r}) = \int \frac{d^2\mathbf{p}}{(2\pi)^2} \mathbf{E}^{0-}(\mathbf{p}) \exp(i\mathbf{k}_p^{0-} \cdot \mathbf{r}) + \int \frac{d^2\mathbf{p}}{(2\pi)^2} \mathbf{E}^{0+}(\mathbf{p}) \exp(i\mathbf{k}_p^{0+} \cdot \mathbf{r}), \quad (3)$$

where (see Fig. 2)

$$\alpha_0(\mathbf{p}) \equiv (\epsilon_0 K_0^2 - \mathbf{p}^2)^{\frac{1}{2}}, \quad (4)$$

$$\mathbf{k}_p^{0\pm} \equiv \mathbf{p} \pm \alpha_0(\mathbf{p}) \hat{e}_z. \quad (5)$$

In fact, when writing such a definition, we made implicitly the assumption that the Rayleigh hypothesis is correct. This representation is only valid when $z > \max[h(\mathbf{x})]$ and in that case $\mathbf{E}^{0-}(\mathbf{p})$ represents the incident wave amplitude. In order to be correct we need to add an explicit dependence in the z coordinate like (see Ref. 25):

$$\mathbf{E}^{0-} = \mathbf{E}^{0-}(\mathbf{p}, z) \quad \mathbf{E}^{0+} = \mathbf{E}^{0+}(\mathbf{p}, z) \quad (6)$$

However, explicit calculations in the case of infinite conducting surfaces,²⁶ and for a dielectric medium⁴ without this hypothesis, have shown that the perturbative developments are identical. The validity of this hypothesis is by no doubt a matter of convergence domain as discussed by Voronovich.^{8,15}

In the medium 1, we have a similar expression :

$$\mathbf{E}^1(\mathbf{r}) = \int \frac{d^2\mathbf{p}}{(2\pi)^2} \mathbf{E}^{1-}(\mathbf{p}) \exp(i\mathbf{k}_p^{1-} \cdot \mathbf{r}) + \int \frac{d^2\mathbf{p}}{(2\pi)^2} \mathbf{E}^{1+}(\mathbf{p}) \exp(i\mathbf{k}_p^{1+} \cdot \mathbf{r}), \quad (7)$$

where

$$\alpha_1(\mathbf{p}) \equiv (\epsilon_1 K_0^2 - \mathbf{p}^2)^{\frac{1}{2}}, \quad (8)$$

$$\mathbf{k}_p^{1\pm} \equiv \mathbf{p} \pm \alpha_1(\mathbf{p}) \hat{\mathbf{e}}_z. \quad (9)$$

We decompose the vectors $\mathbf{E}(\mathbf{p})$ on a two-dimensional basis due to the fact that $\nabla \cdot \mathbf{E}(\mathbf{r}) = 0$, which gives the conditions :

$$\mathbf{k}_p^{0\pm} \cdot \mathbf{E}^{0\pm}(\mathbf{p}) = 0, \quad \mathbf{k}_p^{1\pm} \cdot \mathbf{E}^{1\pm}(\mathbf{p}) = 0. \quad (10)$$

Then, we define the horizontal polarization vectors H for (TE) and V for (TM) in medium 0 by :

$$\hat{\mathbf{e}}_H(\mathbf{p}) \equiv \frac{\hat{\mathbf{e}}_z \times \mathbf{k}_p^{0\pm}}{\|\hat{\mathbf{e}}_z \times \mathbf{k}_p^{0\pm}\|} = \hat{\mathbf{e}}_z \times \hat{\mathbf{p}}, \quad (11)$$

$$\hat{\mathbf{e}}_V^{0\pm}(\mathbf{p}) \equiv \frac{\hat{\mathbf{e}}_H(\mathbf{p}) \times \mathbf{k}_p^{0\pm}}{\|\hat{\mathbf{e}}_H(\mathbf{p}) \times \mathbf{k}_p^{0\pm}\|} = \pm \frac{\alpha_0(\mathbf{p})}{\sqrt{\epsilon_0} K_0} \hat{\mathbf{p}} - \frac{\|\mathbf{p}\|}{\sqrt{\epsilon_0} K_0} \hat{\mathbf{e}}_z, \quad (12)$$

with similar expressions for the medium 1:

$$\hat{\mathbf{e}}_H(\mathbf{p}) \equiv \frac{\hat{\mathbf{e}}_z \times \mathbf{k}_p^{1\pm}}{\|\hat{\mathbf{e}}_z \times \mathbf{k}_p^{1\pm}\|} = \hat{\mathbf{e}}_z \times \hat{\mathbf{p}}, \quad (13)$$

$$\hat{\mathbf{e}}_V^{1\pm}(\mathbf{p}) \equiv \frac{\hat{\mathbf{e}}_H(\mathbf{p}) \times \mathbf{k}_p^{1\pm}}{\|\hat{\mathbf{e}}_H(\mathbf{p}) \times \mathbf{k}_p^{1\pm}\|} = \pm \frac{\alpha_1(\mathbf{p})}{\sqrt{\epsilon_1} K_0} \hat{\mathbf{p}} - \frac{\|\mathbf{p}\|}{\sqrt{\epsilon_1} K_0} \hat{\mathbf{e}}_z. \quad (14)$$

So, we decompose the waves in medium 0 on the basis $[\mathbf{p}]^{0-} \equiv (\hat{\mathbf{e}}_V^{0-}(\mathbf{p}), \hat{\mathbf{e}}_H(\mathbf{p}))$, and $[\mathbf{p}]^{0+} \equiv (\hat{\mathbf{e}}_V^{0+}(\mathbf{p}), \hat{\mathbf{e}}_H(\mathbf{p}))$:

$$\mathbf{E}^{0-}(\mathbf{p}) = \begin{pmatrix} E_V^{0-}(\mathbf{p}) \\ E_H^{0-}(\mathbf{p}) \end{pmatrix}_{[\mathbf{p}]^{0-}}, \quad \mathbf{E}^{0+}(\mathbf{p}) = \begin{pmatrix} E_V^{0+}(\mathbf{p}) \\ E_H^{0+}(\mathbf{p}) \end{pmatrix}_{[\mathbf{p}]^{0+}}, \quad (15)$$

and for medium 1 on the basis $[\mathbf{p}]^{1-} \equiv (\hat{\mathbf{e}}_V^{1-}(\mathbf{p}), \hat{\mathbf{e}}_H(\mathbf{p}))$ and $[\mathbf{p}]^{1+} \equiv (\hat{\mathbf{e}}_V^{1+}(\mathbf{p}), \hat{\mathbf{e}}_H(\mathbf{p}))$:

$$\mathbf{E}^{1-}(\mathbf{p}) = \begin{pmatrix} E_V^{1-}(\mathbf{p}) \\ E_H^{1-}(\mathbf{p}) \end{pmatrix}_{[\mathbf{p}]^{1-}}, \quad \mathbf{E}^{1+}(\mathbf{p}) = \begin{pmatrix} E_V^{1+}(\mathbf{p}) \\ E_H^{1+}(\mathbf{p}) \end{pmatrix}_{[\mathbf{p}]^{1+}}. \quad (16)$$

The electric $\mathbf{E}(\mathbf{x}, z)$ and magnetic fields $\mathbf{B}(\mathbf{x}, z) = \frac{1}{i\omega} \nabla \times \mathbf{E}(\mathbf{x}, z)$, satisfy the following boundary conditions :

$$\mathbf{n}(\mathbf{x}) \times [\mathbf{E}^0(\mathbf{x}, h(\mathbf{x})) - \mathbf{E}^1(\mathbf{x}, h(\mathbf{x}))] = 0, \quad (17)$$

$$\mathbf{n}(\mathbf{x}) \cdot [\epsilon_0 \mathbf{E}^0(\mathbf{x}, h(\mathbf{x})) - \epsilon_1 \mathbf{E}^1(\mathbf{x}, h(\mathbf{x}))] = 0, \quad (18)$$

$$\mathbf{n}(\mathbf{x}) \times [\mathbf{B}^0(\mathbf{x}, h(\mathbf{x})) - \mathbf{B}^1(\mathbf{x}, h(\mathbf{x}))] = 0, \quad (19)$$

$$\mathbf{n}(\mathbf{x}) \equiv \hat{\mathbf{e}}_z - \nabla h(\mathbf{x}).$$

Let us introduce the fields Fourier transform, Eq. (3) and Eq. (7), in the boundary conditions Eqs. (17-19),

they give :

$$\sum_{a=\pm} \int \frac{d^2\mathbf{p}}{(2\pi)^2} \mathbf{n}(\mathbf{x}) \times \mathbf{E}^{0a}(\mathbf{p}) \exp(i\mathbf{k}_\mathbf{p}^{0a} \cdot \mathbf{r}_\mathbf{x}) = \sum_{a=\pm} \int \frac{d^2\mathbf{p}}{(2\pi)^2} \mathbf{n}(\mathbf{x}) \times \mathbf{E}^{1a}(\mathbf{p}) \exp(i\mathbf{k}_\mathbf{p}^{1a} \cdot \mathbf{r}_\mathbf{x}), \quad (20)$$

$$\frac{\epsilon_0}{\epsilon_1} \sum_{a=\pm} \int \frac{d^2\mathbf{p}}{(2\pi)^2} \mathbf{n}(\mathbf{x}) \cdot \mathbf{E}^{0a}(\mathbf{p}) \exp(i\mathbf{k}_\mathbf{p}^{0a} \cdot \mathbf{r}_\mathbf{x}) = \sum_{a=\pm} \int \frac{d^2\mathbf{p}}{(2\pi)^2} \mathbf{n}(\mathbf{x}) \cdot \mathbf{E}^{1a}(\mathbf{p}) \exp(i\mathbf{k}_\mathbf{p}^{1a} \cdot \mathbf{r}_\mathbf{x}), \quad (21)$$

$$\sum_{a=\pm} \int \frac{d^2\mathbf{p}}{(2\pi)^2} \mathbf{n}(\mathbf{x}) \times [\mathbf{k}_\mathbf{p}^{0a} \times \mathbf{E}^{0a}(\mathbf{p})] \exp(i\mathbf{k}_\mathbf{p}^{0a} \cdot \mathbf{r}_\mathbf{x}) = \sum_{a=\pm} \int \frac{d^2\mathbf{p}}{(2\pi)^2} \mathbf{n}(\mathbf{x}) \times [\mathbf{k}_\mathbf{p}^{1a} \times \mathbf{E}^{1a}(\mathbf{p})] \exp(i\mathbf{k}_\mathbf{p}^{1a} \cdot \mathbf{r}_\mathbf{x}), \quad (22)$$

$$\mathbf{r}_\mathbf{x} = \mathbf{x} + h(\mathbf{x})\hat{e}_z, \quad \mathbf{k}_\mathbf{p}^{0a} \equiv \mathbf{p} + a\alpha_0(\mathbf{p})\hat{e}_z, \quad \mathbf{k}_\mathbf{p}^{1a} \equiv \mathbf{p} + a\alpha_1(\mathbf{p})\hat{e}_z, \quad (23)$$

where the summation includes the two possible signs: $a = \pm$, linked to the propagation directions. We will also use the condition $\nabla \cdot \mathbf{E}^0(\mathbf{x}, z) = \nabla \cdot \mathbf{E}^1(\mathbf{x}, z)$, which gives the relation

$$\sum_{a=\pm} \int \frac{d^2\mathbf{p}}{(2\pi)^2} \mathbf{k}_\mathbf{p}^{0a} \cdot \mathbf{E}^{0a}(\mathbf{p}) \exp(i\mathbf{k}_\mathbf{p}^{0a} \cdot \mathbf{r}_\mathbf{x}) = \sum_{a=\pm} \int \frac{d^2\mathbf{p}}{(2\pi)^2} \mathbf{k}_\mathbf{p}^{1a} \cdot \mathbf{E}^{1a}(\mathbf{p}) \exp(i\mathbf{k}_\mathbf{p}^{1a} \cdot \mathbf{r}_\mathbf{x}). \quad (24)$$

B Fields elimination

The equations (20-22) and (24), are all linear in the fields \mathbf{E}^{0-} , \mathbf{E}^{0+} , \mathbf{E}^{1-} , \mathbf{E}^{1+} . In order to eliminate \mathbf{E}^{1-} or \mathbf{E}^{1+} in the equations (20-22) and (24), we will take the following linear combination of their left and right members:

$$\int d^2\mathbf{x} [\mathbf{k}_\mathbf{u}^{1b} \times (Eq. (20)) + (Eq. (22)) - \mathbf{k}_\mathbf{u}^{1b} (Eq. (21)) - \mathbf{n}(\mathbf{x}) (Eq. (24))] \exp(-i\mathbf{k}_\mathbf{u}^{1b} \cdot \mathbf{r}_\mathbf{x}), \quad (25)$$

with $\mathbf{k}_\mathbf{u}^{1b} \equiv \mathbf{u} + b\alpha_1(\mathbf{u})\hat{e}_z$, and where $b = \pm$, has to be fixed according to the choice of the field we want to eliminate. With the vectorial identity, $\mathbf{a} \times (\mathbf{b} \times \mathbf{c}) = \mathbf{b}(\mathbf{a} \cdot \mathbf{c}) - \mathbf{c}(\mathbf{a} \cdot \mathbf{b})$, the right member of Eq. (25) can be written :

$$\sum_{a=\pm} \iint d^2\mathbf{x} \frac{d^2\mathbf{p}}{(2\pi)^2} \left[-(\mathbf{k}_\mathbf{u}^{1b} + \mathbf{k}_\mathbf{p}^{1a}) \cdot \mathbf{n}(\mathbf{x}) \mathbf{E}^{1a}(\mathbf{p}) + (\mathbf{k}_\mathbf{u}^{1b} - \mathbf{k}_\mathbf{p}^{1a}) \cdot \mathbf{E}^{1a}(\mathbf{p}) \mathbf{n}(\mathbf{x}) - \mathbf{n}(\mathbf{x}) \cdot \mathbf{E}^{1a}(\mathbf{p}) (\mathbf{k}_\mathbf{u}^{1b} - \mathbf{k}_\mathbf{p}^{1a}) \right] \exp(-i(\mathbf{k}_\mathbf{u}^{1b} - \mathbf{k}_\mathbf{p}^{1a}) \cdot \mathbf{r}_\mathbf{x}). \quad (26)$$

We have now to discuss the different cases depending on the relative sign between a and b :

1) If $\underline{a = -b}$, we can use an integration by parts (see Appendix A) to evaluate $\mathbf{n}(\mathbf{x}) \equiv \hat{e}_z - \nabla h(\mathbf{x})$. Then we can make the replacement :

$$\mathbf{n}(\mathbf{x}) = \hat{e}_z - \nabla h(\mathbf{x}) \longleftrightarrow \mathbf{n}(\mathbf{x}) = \hat{e}_z + \frac{(\mathbf{u} - \mathbf{p})}{(b\alpha_1(\mathbf{u}) - a\alpha_1(\mathbf{p}))}. \quad (27)$$

It has to be noticed that the denominator $(b\alpha_1(\mathbf{u}) - a\alpha_1(\mathbf{p}))$ does not present any singularity because $a = -b$. For the first term in the integral (26) we obtain:

$$\begin{aligned} -(\mathbf{k}_\mathbf{u}^{1b} + \mathbf{k}_\mathbf{p}^{1a}) \cdot \mathbf{n}(\mathbf{x}) \mathbf{E}^{1a}(\mathbf{p}) &= \frac{-b\mathbf{E}^{1a}(\mathbf{p})}{(\alpha_1(\mathbf{u}) + \alpha_1(\mathbf{p}))} [\mathbf{u}^2 - \mathbf{p}^2 + \alpha_1(\mathbf{u})^2 - \alpha_1(\mathbf{p})^2], \\ &= 0. \end{aligned} \quad (28)$$

The last equality can be easily checked using Eq. (8). For the sum of the second and third terms of Eq. (26), we have also:

$$(\mathbf{k}_\mathbf{u}^{1b} - \mathbf{k}_\mathbf{p}^{1a}) \cdot \mathbf{E}^{1a}(\mathbf{p}) \mathbf{n}(\mathbf{x}) - \mathbf{n}(\mathbf{x}) \cdot \mathbf{E}^{1a}(\mathbf{p}) (\mathbf{k}_\mathbf{u}^{1b} - \mathbf{k}_\mathbf{p}^{1a}) = 0, \quad (29)$$

due to the fact that:

$$\mathbf{n}(\mathbf{x}) = \frac{\mathbf{k}_u^{1b} - \mathbf{k}_p^{1a}}{b\alpha_1(\mathbf{u}) - a\alpha_1(\mathbf{p})}. \quad (30)$$

2) If $\underline{a} = \underline{b}$, we can use again the integration by parts only if $\alpha_1(\mathbf{u}) \neq \alpha_1(\mathbf{p})$. Then we have to consider three cases:

2-a) $\mathbf{u} \neq \mathbf{p}$ and $\mathbf{u} \neq -\mathbf{p}$, as in the previous case by using an integration by parts we show that Eq. (26) is zero.

2-b) $\mathbf{u} = \mathbf{p}$, then $\mathbf{k}_u^{1b} = \mathbf{k}_p^{1a}$:

$$\begin{aligned} - \int d^2\mathbf{x}(\mathbf{k}_u^{1b} + \mathbf{k}_p^{1a}) \cdot \mathbf{n}(\mathbf{x}) \mathbf{E}^{1a}(\mathbf{p}) \exp(-i(\mathbf{k}_u^{1b} - \mathbf{k}_p^{1a}) \cdot \mathbf{r}_x) &= - \int d^2\mathbf{x} 2\mathbf{k}_u^{1b} \cdot \mathbf{n}(\mathbf{x}) \mathbf{E}^{1a}(\mathbf{p}) \\ &= -2b\alpha_1(\mathbf{u}) \int d\mathbf{x} \\ &= -2b\alpha_1(\mathbf{u}) L^2, \end{aligned} \quad (31)$$

because $\int d^2\mathbf{x} \nabla h(\mathbf{x}) = 0$, and

$$(\mathbf{k}_u^{1b} - \mathbf{k}_p^{1a}) \cdot \mathbf{E}^{1a}(\mathbf{p}) \mathbf{n}(\mathbf{x}) - \mathbf{n}(\mathbf{x}) \cdot \mathbf{E}^{1a}(\mathbf{p}) (\mathbf{k}_u^{1b} - \mathbf{k}_p^{1a}) = 0. \quad (32)$$

2-c) $\mathbf{u} = -\mathbf{p} \neq 0$, then $\mathbf{k}_u^{1b} - \mathbf{k}_p^{1a} = 2\mathbf{u}$,

$$\begin{aligned} \int d^2\mathbf{x} \mathbf{n}(\mathbf{x}) \exp(-i(\mathbf{k}_u^{1b} - \mathbf{k}_p^{1a}) \cdot \mathbf{r}_x) &= \int d^2\mathbf{x} (\hat{e}_z - \nabla h(\mathbf{x})) \exp(-2i\mathbf{u} \cdot \mathbf{x}) \\ &= \hat{e}_z \int d^2\mathbf{x} \exp(-2i\mathbf{u} \cdot \mathbf{x}) - \hat{e}_x \int dy [\exp(-2i\mathbf{u} \cdot \mathbf{x}) h(x, y)]_{x=-L/2}^{x=L/2} \\ &\quad - \hat{e}_y \int dx [\exp(-2i\mathbf{u} \cdot \mathbf{x}) h(x, y)]_{y=-L/2}^{y=L/2} \\ &= \hat{e}_z \delta(\mathbf{u}) \quad \text{when } L \rightarrow +\infty \\ &= 0 \quad \text{since } \mathbf{u} \neq 0. \end{aligned} \quad (33)$$

This result implies that the expression (26) is also zero in that case.

We can summarize all the above results in the form :

$$\begin{aligned} - \int d^2\mathbf{x}(\mathbf{k}_u^{1b} + \mathbf{k}_p^{1a}) \cdot \mathbf{n}(\mathbf{x}) \mathbf{E}^{1a}(\mathbf{p}) \exp(-i(\mathbf{k}_u^{1b} - \mathbf{k}_p^{1a}) \cdot \mathbf{r}_x) &= -2b\alpha_1(\mathbf{u}) \delta_{a,b} \delta_{\mathbf{u},\mathbf{p}} L^2 \\ &= -2b\alpha_1(\mathbf{u}) \delta_{a,b} (2\pi)^2 \delta(\mathbf{u} - \mathbf{p}) \mathbf{E}^{1b}(\mathbf{u}) \quad (34) \\ &\text{when } L \rightarrow +\infty, \end{aligned}$$

where $\delta_{\mathbf{u},\mathbf{p}}$ is the kronecker symbol, and $\delta(\mathbf{u} - \mathbf{p}) = (2\pi)^2/L^2 \delta_{\mathbf{u},\mathbf{p}}$ the Dirac function.

After an integration on \mathbf{p} and a summation on a , we obtain for the expression (26):

$$-2b\alpha_1(\mathbf{u}) \mathbf{E}^{1b}(\mathbf{u}). \quad (35)$$

We see that we can eliminate the field $\mathbf{E}^{1-}(\mathbf{u})$ or $\mathbf{E}^{1+}(\mathbf{u})$ depending on the choice made for $b = \pm$.

Now, if we consider the left member of Eq. (25), we have:

$$\begin{aligned} \sum_{a=\pm} \iint d^2\mathbf{x} \frac{d^2\mathbf{p}}{(2\pi)^2} \left[-(\mathbf{k}_u^{1b} + \mathbf{k}_p^{0a}) \cdot \mathbf{n}(\mathbf{x}) \mathbf{E}^{0a}(\mathbf{p}) + (\mathbf{k}_u^{1b} - \mathbf{k}_p^{0a}) \cdot \mathbf{E}^{0a}(\mathbf{p}) \mathbf{n}(\mathbf{x}) \right. \\ \left. - \mathbf{n}(\mathbf{x}) \cdot \mathbf{E}^{0a}(\mathbf{p}) \left(\frac{\epsilon_0}{\epsilon_1} \mathbf{k}_u^{1b} - \mathbf{k}_p^{0a} \right) \right] \exp(-i(\mathbf{k}_u^{1b} - \mathbf{k}_p^{0a}) \cdot \mathbf{r}_x). \end{aligned} \quad (36)$$

Using an integration by parts, we replace $\mathbf{n}(\mathbf{x})$ by (27):

$$\mathbf{n}(\mathbf{x}) \longleftrightarrow \hat{e}_z + \frac{(\mathbf{u} - \mathbf{p})}{(b\alpha_1(\mathbf{u}) - a\alpha_0(\mathbf{p}))} = \frac{\mathbf{k}_u^{1b} - \mathbf{k}_p^{0a}}{(b\alpha_1(\mathbf{u}) - a\alpha_0(\mathbf{p}))}. \quad (37)$$

In this case there is no need to discuss the relative sign between a and b because $b\alpha_1(\mathbf{u}) - a\alpha_0(\mathbf{p}) \neq 0$, due to the fact that $\epsilon_0 \neq \epsilon_1$. We then obtain :

$$\begin{aligned} -(\mathbf{k}_u^{1b} + \mathbf{k}_p^{1a}) \cdot \mathbf{n}(\mathbf{x}) \mathbf{E}^{0a}(\mathbf{p}) &= -\frac{\mathbf{u}^2 - \mathbf{p}^2 + \alpha_1(\mathbf{u})^2 - \alpha_0(\mathbf{p})^2}{b\alpha_1(\mathbf{u}) - a\alpha_0(\mathbf{p})} \mathbf{E}^{0a}(\mathbf{p}), \\ &= -\frac{(\epsilon_1 - \epsilon_0)K_0^2}{b\alpha_1(\mathbf{u}) - a\alpha_0(\mathbf{p})} \mathbf{E}^{0a}(\mathbf{p}), \end{aligned} \quad (38)$$

where we have used the definitions (4) and (8). The remaining terms of Eq. (36) give :

$$\begin{aligned} &(\mathbf{k}_u^{1b} - \mathbf{k}_p^{0a}) \cdot \mathbf{E}^{0a}(\mathbf{p}) \mathbf{n}(\mathbf{x}) - \mathbf{n}(\mathbf{x}) \cdot \mathbf{E}^{0a}(\mathbf{p}) \left(\frac{\epsilon_0}{\epsilon_1} \mathbf{k}_u^{1b} - \mathbf{k}_p^{0a} \right) \\ &= (\mathbf{k}_u^{1b} - \mathbf{k}_p^{0a}) \cdot \mathbf{E}^{0a}(\mathbf{p}) \mathbf{n}(\mathbf{x}) - \mathbf{n}(\mathbf{x}) \cdot \mathbf{E}^{0a}(\mathbf{p}) (\mathbf{k}_u^{1b} - \mathbf{k}_p^{0a}) + \mathbf{n}(\mathbf{x}) \cdot \mathbf{E}^{0a}(\mathbf{p}) \left(\mathbf{k}_u^{1b} - \frac{\epsilon_0}{\epsilon_1} \mathbf{k}_u^{1b} \right) \\ &= \frac{\mathbf{k}_u^{1b} - \mathbf{k}_p^{0a}}{b\alpha_1(\mathbf{u}) - a\alpha_0(\mathbf{p})} \cdot \mathbf{E}^{0a}(\mathbf{p}) \frac{(\epsilon_1 - \epsilon_0)}{\epsilon_1} \mathbf{k}_u^{1b}. \end{aligned} \quad (39)$$

Introducing the following notation :

$$I(\alpha|\mathbf{p}) \equiv \int d^2\mathbf{x} \exp(-i\mathbf{p} \cdot \mathbf{x} - i\alpha h(\mathbf{x})), \quad (40)$$

and taking into account the expressions (35), (38-39), we express the resulting linear combination (25) in the form:

$$\begin{aligned} \sum_{a=\pm} \int \frac{d^2\mathbf{p}}{(2\pi)^2} \frac{I(b\alpha_1(\mathbf{u}) - a\alpha_0(\mathbf{p})|\mathbf{u} - \mathbf{p})}{b\alpha_1(\mathbf{u}) - a\alpha_0(\mathbf{p})} \left[K_0^2 \mathbf{E}^{0a}(\mathbf{p}) - \frac{\mathbf{k}_u^{1b}}{\epsilon_1} (\mathbf{k}_u^{1b} - \mathbf{k}_p^{0a}) \cdot \mathbf{E}^{0a}(\mathbf{p}) \right] \\ = \frac{2b\alpha_1(\mathbf{u})}{(\epsilon_1 - \epsilon_0)} \mathbf{E}^{1b}(\mathbf{u}), \end{aligned} \quad (41)$$

this expression represents in fact a set of two equations, depending on the choice for $b = \pm$. The last step is to project (41) on the natural basis of $\mathbf{E}^{1b}(\mathbf{u})$, namely $[\mathbf{u}]^{1b} \equiv (\hat{\mathbf{e}}_V^{1b}(\mathbf{u}), \hat{\mathbf{e}}_H(\mathbf{u}))$, which has the property to be orthogonal to \mathbf{k}_u^{1b} , so it eliminates the second term of (41) l.h.s. Let us notice that in order to decompose $\mathbf{E}^{0a}(\mathbf{p})$ on $[\mathbf{p}]^{0a}$, one has to define a matrix $\overline{\mathbf{M}}^{1b,0a}(\mathbf{u}|\mathbf{p})$ transforming a vector expressed on the basis $[\mathbf{p}]^{0a}$ into a vector on the basis $[\mathbf{u}]^{1b}$, multiplied by a numerical factor $(\epsilon_0 \epsilon_1)^{\frac{1}{2}} K_0^2$ introduced for a matter of convenience:

$$\overline{\mathbf{M}}^{1b,0a}(\mathbf{u}|\mathbf{p}) \equiv (\epsilon_0 \epsilon_1)^{\frac{1}{2}} K_0^2 \begin{pmatrix} \hat{\mathbf{e}}_V^{1b}(\mathbf{u}) \cdot \hat{\mathbf{e}}_V^{0a}(\mathbf{p}) & \hat{\mathbf{e}}_V^{1b}(\mathbf{u}) \cdot \hat{\mathbf{e}}_H(\mathbf{p}) \\ \hat{\mathbf{e}}_H(\mathbf{u}) \cdot \hat{\mathbf{e}}_V^{0a}(\mathbf{p}) & \hat{\mathbf{e}}_H(\mathbf{u}) \cdot \hat{\mathbf{e}}_H(\mathbf{p}) \end{pmatrix} \quad (42)$$

C The reduced Rayleigh equations

With the definitions (11-14) the matrix $\overline{\mathbf{M}}$ takes the form:

$$\overline{\mathbf{M}}^{1b,0a}(\mathbf{u}|\mathbf{p}) = \begin{pmatrix} \|\mathbf{u}\| \|\mathbf{p}\| + ab\alpha_1(\mathbf{u}) \alpha_0(\mathbf{p}) \hat{\mathbf{u}} \cdot \hat{\mathbf{p}} & -b\epsilon_0^{\frac{1}{2}} K_0 \alpha_1(\mathbf{u}) (\hat{\mathbf{u}} \times \hat{\mathbf{p}})_z \\ a\epsilon_1^{\frac{1}{2}} K_0 \alpha_0(\mathbf{p}) (\hat{\mathbf{u}} \times \hat{\mathbf{p}})_z & (\epsilon_0 \epsilon_1)^{\frac{1}{2}} K_0^2 \hat{\mathbf{u}} \cdot \hat{\mathbf{p}} \end{pmatrix}, \quad (43)$$

and, the two reduced Raleigh equations resulting from Eq. (41) read :

$$\sum_{a=\pm} \int \frac{d^2\mathbf{p}}{(2\pi)^2} \frac{I(b\alpha_1(\mathbf{u}) - a\alpha_0(\mathbf{p})|\mathbf{u} - \mathbf{p})}{b\alpha_1(\mathbf{u}) - a\alpha_0(\mathbf{p})} \overline{\mathbf{M}}^{1b,0a}(\mathbf{u}|\mathbf{p}) \mathbf{E}^{0a}(\mathbf{p}) = \frac{2b(\epsilon_0 \epsilon_1)^{\frac{1}{2}} \alpha_1(\mathbf{u})}{(\epsilon_1 - \epsilon_0)} \mathbf{E}^{1b}(\mathbf{u}), \quad (44)$$

where we suppose that $\mathbf{E}^{0a}(\mathbf{p})$, $\mathbf{E}^{1b}(\mathbf{u})$ are respectively decomposed on the basis $[\mathbf{p}]^{0a}$ and $[\mathbf{u}]^{1b}$. We can derive a similar equation where \mathbf{E}^{0b} is now eliminated, by simply exchanging ϵ_0 and ϵ_1 in (43) and (44), due to the symmetry of the equations (3,7),(17-19), we get :

$$\sum_{a=\pm} \int \frac{d^2\mathbf{p}}{(2\pi)^2} \frac{I(b\alpha_0(\mathbf{u}) - a\alpha_1(\mathbf{p})|\mathbf{u} - \mathbf{p})}{b\alpha_0(\mathbf{u}) - a\alpha_1(\mathbf{p})} \overline{\mathbf{M}}^{0b,1a}(\mathbf{u}|\mathbf{p}) \mathbf{E}^{1a}(\mathbf{p}) = -\frac{2b(\epsilon_0 \epsilon_1)^{\frac{1}{2}} \alpha_0(\mathbf{u})}{(\epsilon_1 - \epsilon_0)} \mathbf{E}^{0b}(\mathbf{u}), \quad (45)$$

$$\overline{\mathbf{M}}^{0b,1a}(\mathbf{u}|\mathbf{p}) = \begin{pmatrix} \|\mathbf{u}\| \|\mathbf{p}\| + ab\alpha_0(\mathbf{u})\alpha_1(\mathbf{p})\hat{\mathbf{u}}\cdot\hat{\mathbf{p}} & -b\epsilon_1^{\frac{1}{2}}K_0\alpha_0(\mathbf{u})(\hat{\mathbf{u}}\times\hat{\mathbf{p}})_z \\ a\epsilon_0^{\frac{1}{2}}K_0\alpha_1(\mathbf{p})(\hat{\mathbf{u}}\times\hat{\mathbf{p}})_z & (\epsilon_0\epsilon_1)^{\frac{1}{2}}K_0^2\hat{\mathbf{u}}\cdot\hat{\mathbf{p}} \end{pmatrix}. \quad (46)$$

In the next sections, we will show how these equations greatly simplify the perturbative calculation of plane waves scattering by a rough surface. In order to keep a compact notation, we introduce new matrices $\overline{\mathbf{M}}_h$ given by :

$$\overline{\mathbf{M}}_h^{1b,0a}(\mathbf{u}|\mathbf{p}) \equiv \frac{I(b\alpha_1(\mathbf{u}) - a\alpha_0(\mathbf{p})|\mathbf{u} - \mathbf{p})}{b\alpha_1(\mathbf{u}) - a\alpha_0(\mathbf{p})} \overline{\mathbf{M}}^{1b,0a}(\mathbf{u}|\mathbf{p}), \quad (47)$$

$$\overline{\mathbf{M}}_h^{0b,1a}(\mathbf{u}|\mathbf{p}) \equiv \frac{I(b\alpha_0(\mathbf{u}) - a\alpha_1(\mathbf{p})|\mathbf{u} - \mathbf{p})}{b\alpha_0(\mathbf{u}) - a\alpha_1(\mathbf{p})} \overline{\mathbf{M}}^{0b,1a}(\mathbf{u}|\mathbf{p}). \quad (48)$$

III. THE DIFFUSION MATRIX

We are interested by the diffusion of an incident plane wave by a rough surface from the previous formalism. We define an incident plane wave of wave vector $\mathbf{k}_{\mathbf{p}_0}^{0-}$ as:

$$\mathbf{E}^{0-}(\mathbf{p}) = (2\pi)^2 \delta(\mathbf{p} - \mathbf{p}_0) \mathbf{E}^i(\mathbf{p}_0). \quad (49)$$

We are naturally led to introduce the diffusion operator $\overline{\mathbf{R}}$:

$$\mathbf{E}^{0+}(\mathbf{p}) \equiv \overline{\mathbf{R}}(\mathbf{p}|\mathbf{p}_0) \cdot \mathbf{E}^i(\mathbf{p}_0), \quad (50)$$

which can be represented in a matrix form, using the vectorial basis described above :

$$\overline{\mathbf{R}}(\mathbf{p}|\mathbf{p}_0) = \begin{pmatrix} R_{VV}(\mathbf{p}|\mathbf{p}_0) & R_{VH}(\mathbf{p}|\mathbf{p}_0) \\ R_{HV}(\mathbf{p}|\mathbf{p}_0) & R_{HH}(\mathbf{p}|\mathbf{p}_0) \end{pmatrix}_{[p_0^-] \rightarrow [p^+]}. \quad (51)$$

The field in medium 0 is now written (using the decomposition (3)):

$$\mathbf{E}^0(\mathbf{r}) = \mathbf{E}^i(\mathbf{p}_0) \exp(i\mathbf{k}_{\mathbf{p}_0}^{0-} \cdot \mathbf{r}) + \int \frac{d^2\mathbf{p}}{(2\pi)^2} \overline{\mathbf{R}}(\mathbf{p}|\mathbf{p}_0) \cdot \mathbf{E}^i(\mathbf{p}_0) \exp(i\mathbf{k}_{\mathbf{p}}^{0+} \cdot \mathbf{r}). \quad (51)$$

IV. A PERTURBATIVE DEVELOPMENT

In order to obtain a perturbative development, one has to make a perturbative analysis of the given boundary-problem. A direct approach which uses an exact integral equation named the extended boundary condition (EBC) (see Ref. 4,26) requires tedious calculations. An other issue is to use the Rayleigh hypothesis in the boundary conditions. This is the method generally used to obtain (SPM)^{12,13,15}. But a great deal of simplifications can be achieved if we are only interested by the field outside the slab. It was discovered by Brown *et al.*¹⁶, that an exact integral equation can be obtained (excepted for the Rayleigh hypothesis), which only involves the scattering matrix $\overline{\mathbf{R}}(\mathbf{p}|\mathbf{p}_0)$. The proof is based on the extinction theorem which decouples the fields inside and outside the media. In this section, we will show how to obtain this integral equation from the previous development, including a generalization to the case of bounded random media. We seek for a perturbative development of $\overline{\mathbf{R}}$ in power of the height h :

$$\overline{\mathbf{R}}(\mathbf{p}|\mathbf{p}_0) = \overline{\mathbf{R}}^{(0)}(\mathbf{p}|\mathbf{p}_0) + \overline{\mathbf{R}}^{(1)}(\mathbf{p}|\mathbf{p}_0) + \overline{\mathbf{R}}^{(2)}(\mathbf{p}|\mathbf{p}_0) + \overline{\mathbf{R}}^{(3)}(\mathbf{p}|\mathbf{p}_0) + \dots \quad (52)$$

One can easily prove, that this development takes the following form (see Appendix B):

$$\begin{aligned} \overline{\mathbf{R}}(\mathbf{p}|\mathbf{p}_0) &= (2\pi)^2 \delta(\mathbf{p} - \mathbf{p}_0) \overline{\mathbf{X}}^{(0)}(\mathbf{p}_0) + \alpha_0(\mathbf{p}_0) \overline{\mathbf{X}}^{(1)}(\mathbf{p}|\mathbf{p}_0) h(\mathbf{p} - \mathbf{p}_0) \\ &+ \alpha_0(\mathbf{p}_0) \int \frac{d^2\mathbf{p}_1}{(2\pi)^2} \overline{\mathbf{X}}^{(2)}(\mathbf{p}|\mathbf{p}_1|\mathbf{p}_0) h(\mathbf{p} - \mathbf{p}_1) h(\mathbf{p}_1 - \mathbf{p}_0) \\ &+ \alpha_0(\mathbf{p}_0) \iint \frac{d^2\mathbf{p}_1}{(2\pi)^2} \frac{d^2\mathbf{p}_2}{(2\pi)^2} \overline{\mathbf{X}}^{(3)}(\mathbf{p}|\mathbf{p}_1|\mathbf{p}_2|\mathbf{p}_0) h(\mathbf{p} - \mathbf{p}_1) h(\mathbf{p}_1 - \mathbf{p}_2) h(\mathbf{p}_2 - \mathbf{p}_0), \end{aligned} \quad (53)$$

where $h(\mathbf{p})$ is the Fourier transform³³ of $h(\mathbf{x})$:

$$h(\mathbf{p}) \equiv \int d^2\mathbf{x} \exp(-i\mathbf{p} \cdot \mathbf{x}) h(\mathbf{x}). \quad (54)$$

We will now exemplify the power of the reduced Rayleigh equation for the three configurations mentioned in the introduction.

A A rough surface separating two different media

We consider a rough surface delimiting two media which are semi infinite, see Fig. 3. We suppose that there is no upward field propagating in the medium 1, so $\mathbf{E}^{1+} = 0$. With the choice, $b = +$, in equation (44), we obtain the following integral equation for the scattering matrix $\overline{\mathbf{R}}_{s\epsilon_0, \epsilon_1}(\mathbf{p}|\mathbf{p}_0)$ for a single surface³⁴ (the subscript s means a single surface located at $z = 0$)

$$\int \frac{d^2\mathbf{p}}{(2\pi)^2} \overline{\mathbf{M}}_h^{1+,0+}(\mathbf{u}|\mathbf{p}) \cdot \overline{\mathbf{R}}_{s\epsilon_0, \epsilon_1}(\mathbf{p}|\mathbf{p}_0) + \overline{\mathbf{M}}_h^{1+,0-}(\mathbf{u}|\mathbf{p}_0) = 0 \quad (55)$$

(This equation has been already obtained making use of the extinction theorem.¹⁶ It has to be noticed that since the r.h.s of (55) is null, one can simplify the second ligh of the matrices, $\overline{\mathbf{M}}^{1+,0+}, \overline{\mathbf{M}}^{1+,0-}$, by a factor $(\epsilon_1)^{\frac{1}{2}}$, then they coincide with the $\overline{\mathbf{M}}, \overline{\mathbf{N}}$ matrices derived by Celli *et al*¹⁶.)

In order to construct a perturbative development, the method is simply to expand in Taylor series the term $\exp(i\alpha h(\mathbf{x}))$ inside $I(\alpha|\mathbf{p})$, (Eq. (40)) :

$$I(\alpha|\mathbf{p}) = (2\pi)^2 \delta(\mathbf{p}) - i\alpha h^{(1)}(\mathbf{p}) - \frac{\alpha^2}{2} h^{(2)}(\mathbf{p}) - \frac{i\alpha^3}{3!} h^{(3)}(\mathbf{p}) + \dots, \quad (56)$$

$$h^{(n)}(\mathbf{p}) \equiv \int d^2\mathbf{x} \exp(-i\mathbf{p} \cdot \mathbf{x}) h^n(\mathbf{x}), \quad (57)$$

and, to collect the terms of the same order in $h(\mathbf{x})$. Let us define the matrix

$$\overline{\mathbf{D}}_{10}^{\pm}(\mathbf{p}_0) \equiv \begin{pmatrix} \epsilon_1 \alpha_0(\mathbf{p}_0) \pm \epsilon_0 \alpha_1(\mathbf{p}_0) & 0 \\ 0 & \alpha_0(\mathbf{p}_0) \pm \alpha_1(\mathbf{p}_0) \end{pmatrix}, \quad (58)$$

the classical specular reflection coefficients for (TM) and (TE) waves are given by the diagonal elements of the matrix

$$\overline{\mathbf{V}}^{10}(\mathbf{p}_0) \equiv \overline{\mathbf{D}}_{10}^{-}(\mathbf{p}_0) \cdot \left[\overline{\mathbf{D}}_{10}^{+}(\mathbf{p}_0) \right]^{-1}. \quad (59)$$

Introducing (56) in (55), we obtain for $\overline{\mathbf{R}}_{s\epsilon_0, \epsilon_1}$ a perturbative development of the form (53), where the coefficients are given by:

$$\begin{aligned} \overline{\mathbf{X}}_{s\epsilon_0, \epsilon_1}^{(0)}(\mathbf{p}_0) &= -\frac{\alpha_1(\mathbf{p}_0) - \alpha_0(\mathbf{p}_0)}{\alpha_1(\mathbf{p}_0) + \alpha_0(\mathbf{p}_0)} [\overline{\mathbf{M}}^{1+,0+}(\mathbf{p}_0|\mathbf{p}_0)]^{-1} \cdot \overline{\mathbf{M}}^{1+,0-}(\mathbf{p}_0|\mathbf{p}_0) \\ &= \overline{\mathbf{V}}^{10}(\mathbf{p}_0), \end{aligned} \quad (60)$$

and

$$\overline{\mathbf{X}}_{s\epsilon_0, \epsilon_1}^{(1)}(\mathbf{u}|\mathbf{p}_0) = 2i \overline{\mathbf{Q}}^+(\mathbf{u}|\mathbf{p}_0), \quad (61)$$

$$\overline{\mathbf{X}}_{s\epsilon_0, \epsilon_1}^{(2)}(\mathbf{u}|\mathbf{p}_1|\mathbf{p}_0) = \alpha_1(\mathbf{u}) \overline{\mathbf{Q}}^+(\mathbf{u}|\mathbf{p}_0) + \alpha_0(\mathbf{p}_0) \overline{\mathbf{Q}}^-(\mathbf{u}|\mathbf{p}_0) - 2 \overline{\mathbf{P}}(\mathbf{u}|\mathbf{p}_1) \cdot \overline{\mathbf{Q}}^+(\mathbf{p}_1|\mathbf{p}_0), \quad (62)$$

$$\begin{aligned} \overline{\mathbf{X}}_{s\epsilon_0, \epsilon_1}^{(3)}(\mathbf{u}|\mathbf{p}_1|\mathbf{p}_2|\mathbf{p}_0) &= -\frac{i}{3} \left[(\alpha_1^2(\mathbf{u}) + \alpha_0^2(\mathbf{p}_0)) \overline{\mathbf{Q}}^+(\mathbf{u}|\mathbf{p}_0) + 2 \alpha_1(\mathbf{u}) \alpha_0(\mathbf{p}_0) \overline{\mathbf{Q}}^-(\mathbf{u}|\mathbf{p}_0) \right] \\ &\quad + i \overline{\mathbf{P}}(\mathbf{u}|\mathbf{p}_1) \overline{\mathbf{X}}_{s\epsilon_0, \epsilon_1}^{(2)}(\mathbf{p}_1|\mathbf{p}_2|\mathbf{p}_0) + i (\alpha_1(\mathbf{u}) - \alpha_0(\mathbf{p}_2)) \cdot \overline{\mathbf{P}}(\mathbf{u}|\mathbf{p}_2) \cdot \overline{\mathbf{Q}}^+(\mathbf{p}_2|\mathbf{p}_0), \end{aligned} \quad (63)$$

with

$$\overline{Q}^{\pm}(\mathbf{u}|\mathbf{p}_0) \equiv \frac{\alpha_1(\mathbf{u}) - \alpha_0(\mathbf{u})}{2\alpha_0(\mathbf{p}_0)} [\overline{M}^{1+,0+}(\mathbf{u}|\mathbf{u})]^{-1} \cdot [\overline{M}^{1+,0-}(\mathbf{u}|\mathbf{p}_0) \pm \overline{M}^{1+,0+}(\mathbf{u}|\mathbf{p}_0) \cdot \overline{X}^{(0)}(\mathbf{p}_0)], \quad (64)$$

$$\overline{P}(\mathbf{u}|\mathbf{p}_1) \equiv (\alpha_1(\mathbf{u}) - \alpha_0(\mathbf{u})) [\overline{M}^{1+,0+}(\mathbf{u}|\mathbf{u})]^{-1} \cdot \overline{M}^{1+,0+}(\mathbf{u}|\mathbf{p}_1) \quad (65)$$

and, after some simple algebra we obtain:

$$\overline{Q}^+(\mathbf{u}|\mathbf{p}_0) = (\epsilon_1 - \epsilon_0) [\overline{D}_{10}^+(\mathbf{u})]^{-1} \cdot \begin{pmatrix} \epsilon_1 \|\mathbf{u}\| \|\mathbf{p}_0\| - \epsilon_0 \alpha_1(\mathbf{u}) \alpha_1(\mathbf{p}_0) \hat{\mathbf{u}} \cdot \hat{\mathbf{p}}_0 & -\epsilon_0^{\frac{1}{2}} K_0 \alpha_1(\mathbf{u}) (\hat{\mathbf{u}} \times \hat{\mathbf{p}}_0)_z \\ -\epsilon_0^{\frac{1}{2}} K_0 \alpha_1(\mathbf{p}_0) (\hat{\mathbf{u}} \times \hat{\mathbf{p}}_0)_z & K_0^2 \hat{\mathbf{u}} \cdot \hat{\mathbf{p}}_0 \end{pmatrix} \cdot [\overline{D}_{10}^+(\mathbf{p}_0)]^{-1}, \quad (66)$$

$$\overline{Q}^-(\mathbf{u}|\mathbf{p}_0) = \frac{(\epsilon_1 - \epsilon_0)}{\alpha_0(\mathbf{p}_0)} [\overline{D}_{10}^+(\mathbf{u})]^{-1} \cdot \begin{pmatrix} \epsilon_0 \alpha_1(\mathbf{p}_0) \|\mathbf{u}\| \|\mathbf{p}_0\| - \epsilon_1 \alpha_1(\mathbf{u}) \alpha_0^2(\mathbf{p}_0) \hat{\mathbf{u}} \cdot \hat{\mathbf{p}}_0 & -\epsilon_0^{\frac{1}{2}} K_0 \alpha_1(\mathbf{u}) \alpha_1(\mathbf{p}_0) (\hat{\mathbf{u}} \times \hat{\mathbf{p}}_0)_z \\ -\epsilon_0^{-\frac{1}{2}} \epsilon_1 K_0 \alpha_0^2(\mathbf{p}_0) (\hat{\mathbf{u}} \times \hat{\mathbf{p}}_0)_z & K_0^2 \alpha_1(\mathbf{p}_0) \hat{\mathbf{u}} \cdot \hat{\mathbf{p}}_0 \end{pmatrix} \cdot [\overline{D}_{10}^+(\mathbf{p}_0)]^{-1}, \quad (67)$$

$$\overline{P}(\mathbf{u}|\mathbf{p}_1) = (\epsilon_1 - \epsilon_0) [\overline{D}_{10}^+(\mathbf{u})]^{-1} \cdot \begin{pmatrix} \|\mathbf{u}\| \|\mathbf{p}_1\| + \alpha_1(\mathbf{u}) \alpha_0(\mathbf{p}_1) \hat{\mathbf{u}} \cdot \hat{\mathbf{p}}_1 & -\epsilon_0^{\frac{1}{2}} K_0 \alpha_1(\mathbf{u}) (\hat{\mathbf{u}} \times \hat{\mathbf{p}}_1)_z \\ \epsilon_0^{-\frac{1}{2}} K_0 \alpha_0(\mathbf{p}_1) (\hat{\mathbf{u}} \times \hat{\mathbf{p}}_1)_z & K_0^2 \hat{\mathbf{u}} \cdot \hat{\mathbf{p}}_1 \end{pmatrix}. \quad (68)$$

It can be easily checked that $\overline{X}^{(1)}$ is the well known first order term in perturbation theory which was obtained by Rice.¹² After some lengthy calculations, we have proven that Eqs. (62,63), are identical to those found by Johnson.¹³ Thus our expressions (62), (63), are a compact manner to write the second and third order terms of the perturbative expansion, moreover, they are well adapted for numerical computations. However, it has to be noticed that only the first term $\overline{X}^{(1)}$ is reciprocal. Since the second and third-order perturbative terms are included in an integral, the coefficient $\overline{X}^{(2)}$, $\overline{X}^{(3)}$, are not unique, however they can be put into a reciprocal form (see Appendix B).

It is worth to notice that we can follow an analogous procedure to calculate the transmitted field. By taking $b = -$ in Eq. (45), we get:

$$\int \frac{d^2\mathbf{p}}{(2\pi)^2} \overline{M}_h^{0-,1-}(\mathbf{u}|\mathbf{p}) \cdot \mathbf{E}^{1-}(\mathbf{p}) = \frac{2(\epsilon_0 \epsilon_1)^{\frac{1}{2}} \alpha_0(\mathbf{u})}{(\epsilon_1 - \epsilon_0)} \mathbf{E}^{0-}(\mathbf{u}). \quad (69)$$

This equation was already obtained with the extinction theorem.²⁴

B A slab with a rough surface on the bottom side

We consider a slab delimited on the upper side by a planar surface and on the bottom side by a rough surface, see Fig. 4. Since there is no incident upward field in medium 2, the scattering matrix obtained in the preceding section is sufficient to determine the scattering matrix of the present configuration. In order to get a proof, let us introduce some definitions as explained in Fig. 5. The scattering matrix for an incident plane wave coming from the medium 0, and scattered in the medium 1 is given by:

$$\overline{V}^0(\mathbf{p}|\mathbf{p}_0) = (2\pi)^2 \delta(\mathbf{p} - \mathbf{p}_0) \overline{V}^{10}(\mathbf{p}_0), \quad (70)$$

where \overline{V}^{10} is defined by (59). The transmitted wave in the medium 1 is given by:

$$\overline{T}^0(\mathbf{p}|\mathbf{p}_0) = (2\pi)^2 \delta(\mathbf{p} - \mathbf{p}_0) \frac{\alpha_0(\mathbf{p}_0)}{\alpha_1(\mathbf{p}_0)} \overline{T}^{10}(\mathbf{p}_0), \quad (71)$$

$$\overline{T}^{10}(\mathbf{p}_0) \equiv 2\alpha_1(\mathbf{p}_0) \begin{pmatrix} (\epsilon_0 \epsilon_1)^{\frac{1}{2}} & 0 \\ 0 & 1 \end{pmatrix} \cdot [\overline{D}_{10}^+(\mathbf{p}_0)]^{-1}. \quad (72)$$

Now, when the incident wave is coming from the medium 1, we have similarly :

$$\overline{\mathbf{V}}^1(\mathbf{p}|\mathbf{p}_0) = -(2\pi)^2 \delta(\mathbf{p} - \mathbf{p}_0) \overline{\mathbf{V}}^{10}(\mathbf{p}_0), \quad (73)$$

$$\overline{\mathbf{T}}^1(\mathbf{p}|\mathbf{p}_0) = (2\pi)^2 \delta(\mathbf{p} - \mathbf{p}_0) \overline{\mathbf{T}}^{10}(\mathbf{p}_0). \quad (74)$$

The scattering matrix $\overline{\mathbf{R}}_{s\epsilon_1, \epsilon_2}^H$ for the rough surface h which is located at $z = -H$ ³⁵, and separating two media of permittivity ϵ_1 and ϵ_2 is given by:

$$\overline{\mathbf{R}}_{s\epsilon_1, \epsilon_2}^H(\mathbf{p}|\mathbf{p}_0) = \exp(i(\alpha_1(\mathbf{p}) + \alpha_1(\mathbf{p}_0))H) \overline{\mathbf{R}}_{s\epsilon_1, \epsilon_2}(\mathbf{p}|\mathbf{p}_0), \quad (75)$$

where the phase term comes from the translation $z = -H$, (see (B2)), and $\overline{\mathbf{R}}_{s\epsilon_1, \epsilon_2}$ denotes the scattering matrix $\overline{\mathbf{R}}_{s\epsilon_0, \epsilon_1}$ of the previous section, where we have replaced ϵ_0 by ϵ_1 , and ϵ_1 by ϵ_2 . Furthermore, if we define the product of two operator $\overline{\mathbf{A}}$ and $\overline{\mathbf{B}}$ by:

$$(\overline{\mathbf{A}} \cdot \overline{\mathbf{B}})(\mathbf{p}|\mathbf{p}_0) \equiv \int \frac{d^2\mathbf{p}_1}{(2\pi)^2} \overline{\mathbf{A}}(\mathbf{p}|\mathbf{p}_1) \cdot \overline{\mathbf{B}}(\mathbf{p}_1|\mathbf{p}_0), \quad (76)$$

one can easily prove for the configuration shown in Fig. 4 that (we use for the fields the notations of Fig. 1),

$$\mathbf{E}^{1+} = \overline{\mathbf{R}}_{s\epsilon_1, \epsilon_2}^H \cdot \overline{\mathbf{T}}^0 \cdot \mathbf{E}^{0-} + \overline{\mathbf{R}}_{s\epsilon_1, \epsilon_2}^H \cdot \overline{\mathbf{V}}^1 \cdot \mathbf{E}^{1+}, \quad (77)$$

$$\mathbf{E}^{0+} = \overline{\mathbf{V}}^0 \cdot \mathbf{E}^{0-} + \overline{\mathbf{T}}^1 \cdot \mathbf{E}^{1+}, \quad (78)$$

where $\mathbf{E}^{0-}(\mathbf{p}) = (2\pi)^2 \delta(\mathbf{p} - \mathbf{p}_0) \mathbf{E}^i(\mathbf{p}_0)$. These equations have been recently used to calculate in the first order the field scattered by a layered medium.¹⁴ In fact, as we shall see below, these equations allow us to obtain all orders of the field perturbation. The expression (77) is analogous to the Dyson equation usually used in random media.⁴ So, we are naturally led to introduce a scattering operator $\overline{\mathbf{U}}$:

$$\mathbf{E}^{1+} = \overline{\mathbf{R}}_{s\epsilon_1, \epsilon_2}^H \cdot \overline{\mathbf{U}} \cdot \overline{\mathbf{T}}^0 \cdot \mathbf{E}^{0-}, \quad (79)$$

which satisfies the equation

$$\overline{\mathbf{U}} = \overline{\mathbf{I}} + \overline{\mathbf{V}}^1 \cdot \overline{\mathbf{R}}_{s\epsilon_1, \epsilon_2}^H \cdot \overline{\mathbf{U}}. \quad (80)$$

If we define by $\overline{\mathbf{R}}_d(\mathbf{p}|\mathbf{p}_0)$ the global scattering matrix for the upper planar surface and the bottom rough surface by,

$$\mathbf{E}^{0+}(\mathbf{p}) = \overline{\mathbf{R}}_d(\mathbf{p}|\mathbf{p}_0) \cdot \mathbf{E}^i(\mathbf{p}_0), \quad (81)$$

with Eqs. (78,79), the scattering matrix becomes:

$$\overline{\mathbf{R}}_d = \overline{\mathbf{V}}^0 + \overline{\mathbf{T}}^1 \cdot \overline{\mathbf{R}}_{s\epsilon_1, \epsilon_2}^H \cdot \overline{\mathbf{U}} \cdot \overline{\mathbf{T}}^0. \quad (82)$$

We can improve the development (80), by summing all the specular reflexions inside the slab, this can be done by introducing the operator $\overline{\mathbf{U}}^{(0)}$ which satisfies the equation

$$\overline{\mathbf{U}}^{(0)} = \overline{\mathbf{I}} + \overline{\mathbf{V}}^1 \cdot \overline{\mathbf{R}}_{s\epsilon_1, \epsilon_2}^{H(0)} \cdot \overline{\mathbf{U}}^{(0)}, \quad (83)$$

where $\overline{\mathbf{R}}_{s\epsilon_1, \epsilon_2}^{H(0)}$ is the zeroth order term of the perturbative development which is given by:

$$\overline{\mathbf{R}}_{s\epsilon_1, \epsilon_2}^{H(0)}(\mathbf{p}|\mathbf{p}_0) = (2\pi)^2 \delta(\mathbf{p} - \mathbf{p}_0) \overline{\mathbf{V}}^{H21}(\mathbf{p}_0), \quad (84)$$

and, $\overline{\mathbf{V}}^{H21}$ is the scattering matrix for a planar surface located at the height $z = -H$

$$\overline{\mathbf{V}}^{H21}(\mathbf{u}) \equiv \exp(2i\alpha_1(\mathbf{u})H) \overline{\mathbf{D}}_{21}^-(\mathbf{p}_0) \cdot \left[\overline{\mathbf{D}}_{21}^+(\mathbf{p}_0) \right]^{-1}, \quad (85)$$

$$\overline{\mathbf{D}}_{21}^\pm(\mathbf{p}_0) \equiv \begin{pmatrix} \epsilon_2 \alpha_1(\mathbf{p}_0) \pm \epsilon_1 \alpha_2(\mathbf{p}_0) & 0 \\ 0 & \alpha_1(\mathbf{p}_0) \pm \alpha_2(\mathbf{p}_0) \end{pmatrix}. \quad (86)$$

The term $\exp(2i\alpha_1(\mathbf{u})H)$ comes from the phase shift induced by the translation of the planar surface from the height $z = 0$ to $z = -H$ (see Appendix B2). The diagrammatic representation of Eq. (83) is shown in Fig. 6, it is in fact a geometric series which can be summed

$$\overline{\mathbf{U}}^{(0)}(\mathbf{p}|\mathbf{p}_0) = (2\pi)^2 \delta(\mathbf{p} - \mathbf{p}_0) \overline{\mathbf{U}}^{(0)}(\mathbf{p}_0), \quad (87)$$

$$\overline{\mathbf{U}}^{(0)}(\mathbf{p}_0) \equiv \left[\overline{\mathbf{1}} + \overline{\mathbf{V}}^{10}(\mathbf{p}_0) \cdot \overline{\mathbf{V}}^{H21}(\mathbf{p}_0) \right]^{-1}. \quad (88)$$

From the previous results, Eq. (80) can be written in the following form :

$$\overline{\mathbf{U}} = \overline{\mathbf{U}}^{(0)} + \overline{\mathbf{U}}^{(0)} \cdot \overline{\mathbf{V}}^1 \cdot \Delta \overline{\mathbf{R}}_{s\epsilon_1, \epsilon_2}^H \cdot \overline{\mathbf{U}}, \quad (89)$$

where

$$\Delta \overline{\mathbf{R}}_{s\epsilon_1, \epsilon_2}^H \equiv \overline{\mathbf{R}}_{s\epsilon_1, \epsilon_2}^H - \overline{\mathbf{R}}_{s\epsilon_1, \epsilon_2}^{H(0)}. \quad (90)$$

In order to obtain the perturbative development of $\overline{\mathbf{R}}_d$, we introduce the expansion

$$\overline{\mathbf{R}}_{s\epsilon_1, \epsilon_2}^H = \overline{\mathbf{R}}_{s\epsilon_1, \epsilon_2}^{H(0)} + \overline{\mathbf{R}}_{s\epsilon_1, \epsilon_2}^{H(1)} + \overline{\mathbf{R}}_{s\epsilon_1, \epsilon_2}^{H(2)} + \overline{\mathbf{R}}_{s\epsilon_1, \epsilon_2}^{H(3)}, \quad (91)$$

in (82) and (89), which gives the following terms

$$\overline{\mathbf{R}}_d^{(0)} = \overline{\mathbf{V}}^0 + \overline{\mathbf{T}}^1 \cdot \overline{\mathbf{R}}_{s\epsilon_1, \epsilon_2}^{H(0)} \cdot \overline{\mathbf{U}}^{(0)} \cdot \overline{\mathbf{T}}^0, \quad (92)$$

$$\overline{\mathbf{R}}_d^{(1)} = \overline{\mathbf{T}}^1 \cdot \overline{\mathbf{U}}^{(0)} \cdot \overline{\mathbf{R}}_{s\epsilon_1, \epsilon_2}^{H(1)} \cdot \overline{\mathbf{U}}^{(0)} \cdot \overline{\mathbf{T}}^0, \quad (93)$$

$$\overline{\mathbf{R}}_d^{(2)} = \overline{\mathbf{T}}^1 \cdot \overline{\mathbf{U}}^{(0)} \cdot \left[\overline{\mathbf{R}}_{s\epsilon_1, \epsilon_2}^{H(2)} + \overline{\mathbf{R}}_{s\epsilon_1, \epsilon_2}^{H(1)} \cdot \overline{\mathbf{U}}^{(0)} \cdot \overline{\mathbf{V}}^1 \cdot \overline{\mathbf{R}}_{s\epsilon_1, \epsilon_2}^{H(1)} \right] \cdot \overline{\mathbf{U}}^{(0)} \cdot \overline{\mathbf{T}}^0, \quad (94)$$

$$\begin{aligned} \overline{\mathbf{R}}_d^{(3)} = & \overline{\mathbf{T}}^1 \cdot \overline{\mathbf{U}}^{(0)} \cdot \left[\overline{\mathbf{R}}_{s\epsilon_1, \epsilon_2}^{H(3)} + \overline{\mathbf{R}}_{s\epsilon_1, \epsilon_2}^{H(2)} \cdot \overline{\mathbf{U}}^{(0)} \cdot \overline{\mathbf{V}}^1 \cdot \overline{\mathbf{R}}_{s\epsilon_1, \epsilon_2}^{H(1)} + \overline{\mathbf{R}}_{s\epsilon_1, \epsilon_2}^{H(1)} \cdot \overline{\mathbf{U}}^{(0)} \cdot \overline{\mathbf{V}}^1 \cdot \overline{\mathbf{R}}_{s\epsilon_1, \epsilon_2}^{H(2)} \right. \\ & \left. + \overline{\mathbf{R}}_{s\epsilon_1, \epsilon_2}^{H(1)} \cdot \overline{\mathbf{U}}^{(0)} \cdot \overline{\mathbf{V}}^1 \cdot \overline{\mathbf{R}}_{s\epsilon_1, \epsilon_2}^{H(1)} \cdot \overline{\mathbf{U}}^{(0)} \cdot \overline{\mathbf{V}}^1 \cdot \overline{\mathbf{R}}_{s\epsilon_1, \epsilon_2}^{H(1)} \right] \cdot \overline{\mathbf{U}}^{(0)} \cdot \overline{\mathbf{T}}^0. \end{aligned} \quad (95)$$

Using the development (53) for $\overline{\mathbf{R}}_{s\epsilon_1, \epsilon_2}^H$, and the definitions (70-71), (73-74), we obtain after some calculations a development of the form (53) for $\overline{\mathbf{R}}_d$ with the following coefficients:

$$\overline{\mathbf{X}}_d^{(0)}(\mathbf{p}_0) = \left(\overline{\mathbf{V}}^{10}(\mathbf{p}_0) + \overline{\mathbf{V}}^{H21}(\mathbf{p}_0) \right) \cdot \left[\overline{\mathbf{1}} + \overline{\mathbf{V}}^{10}(\mathbf{p}_0) \cdot \overline{\mathbf{V}}^{H21}(\mathbf{p}_0) \right]^{-1}, \quad (96)$$

this matrix is naturally diagonal, and its coefficients are identical to those of the reflection coefficients for a planar slab⁴. The other coefficients are

$$\overline{\mathbf{X}}_d^{(1)}(\mathbf{p}|\mathbf{p}_0) = \overline{\mathbf{T}}^{10}(\mathbf{p}) \cdot \overline{\mathbf{U}}^{(0)}(\mathbf{p}) \cdot \overline{\mathbf{X}}_{s\epsilon_1, \epsilon_2}^{H(1)}(\mathbf{p}|\mathbf{p}_0) \cdot \overline{\mathbf{U}}^{(0)}(\mathbf{p}_0) \cdot \overline{\mathbf{T}}^{10}(\mathbf{p}_0), \quad (97)$$

$$\begin{aligned} \overline{\mathbf{X}}_d^{(2)}(\mathbf{p}|\mathbf{p}_1|\mathbf{p}_0) = & \overline{\mathbf{T}}^{10}(\mathbf{p}) \cdot \overline{\mathbf{U}}^{(0)}(\mathbf{p}) \cdot \left[\overline{\mathbf{X}}_{s\epsilon_1, \epsilon_2}^{H(2)}(\mathbf{p}|\mathbf{p}_1|\mathbf{p}_0) \right. \\ & \left. - \alpha_1(\mathbf{p}_1) \overline{\mathbf{X}}_{s\epsilon_1, \epsilon_2}^{H(1)}(\mathbf{p}|\mathbf{p}_1) \cdot \overline{\mathbf{U}}^{(0)}(\mathbf{p}_1) \cdot \overline{\mathbf{V}}^{10}(\mathbf{p}_1) \cdot \overline{\mathbf{X}}_{s\epsilon_1, \epsilon_2}^{H(1)}(\mathbf{p}_1|\mathbf{p}_0) \right] \cdot \overline{\mathbf{U}}^{(0)}(\mathbf{p}_0) \cdot \overline{\mathbf{T}}^{10}(\mathbf{p}_0), \end{aligned} \quad (98)$$

$$\begin{aligned} \overline{\mathbf{X}}_d^{(3)}(\mathbf{p}|\mathbf{p}_1|\mathbf{p}_2|\mathbf{p}_0) = & \overline{\mathbf{T}}^{10}(\mathbf{p}) \cdot \overline{\mathbf{U}}^{(0)}(\mathbf{p}) \cdot \left[\overline{\mathbf{X}}_{s\epsilon_1, \epsilon_2}^{H(3)}(\mathbf{p}|\mathbf{p}_1|\mathbf{p}_2|\mathbf{p}_0) \right. \\ & - \alpha_1(\mathbf{p}_2) \overline{\mathbf{X}}_{s\epsilon_1, \epsilon_2}^{H(2)}(\mathbf{p}|\mathbf{p}_1|\mathbf{p}_2) \cdot \overline{\mathbf{U}}^{(0)}(\mathbf{p}_2) \cdot \overline{\mathbf{V}}^{10}(\mathbf{p}_2) \cdot \overline{\mathbf{X}}_{s\epsilon_1, \epsilon_2}^{H(1)}(\mathbf{p}_2|\mathbf{p}_0) \\ & - \alpha_1(\mathbf{p}_1) \overline{\mathbf{X}}_{s\epsilon_1, \epsilon_2}^{H(1)}(\mathbf{p}|\mathbf{p}_1) \cdot \overline{\mathbf{U}}^{(0)}(\mathbf{p}_1) \cdot \overline{\mathbf{V}}^{10}(\mathbf{p}_1) \cdot \overline{\mathbf{X}}_{s\epsilon_1, \epsilon_2}^{H(2)}(\mathbf{p}_1|\mathbf{p}_2|\mathbf{p}_0) \\ & + \alpha_1(\mathbf{p}_1) \alpha_1(\mathbf{p}_2) \overline{\mathbf{X}}_{s\epsilon_1, \epsilon_2}^{H(1)}(\mathbf{p}|\mathbf{p}_1) \cdot \overline{\mathbf{U}}^{(0)}(\mathbf{p}_1) \cdot \overline{\mathbf{V}}^{10}(\mathbf{p}_1) \cdot \overline{\mathbf{X}}_{s\epsilon_1, \epsilon_2}^{H(1)}(\mathbf{p}_1|\mathbf{p}_2) \\ & \left. \cdot \overline{\mathbf{U}}^{(0)}(\mathbf{p}_2) \cdot \overline{\mathbf{V}}^{10}(\mathbf{p}_2) \cdot \overline{\mathbf{X}}_{s\epsilon_1, \epsilon_2}^{H(1)}(\mathbf{p}_2|\mathbf{p}_0) \right] \cdot \overline{\mathbf{U}}^{(0)}(\mathbf{p}_0) \cdot \overline{\mathbf{T}}^{10}(\mathbf{p}_0). \end{aligned} \quad (99)$$

In these expressions, $\overline{\mathbf{X}}_{s\epsilon_1, \epsilon_2}^{H(n)}(\mathbf{p}|\mathbf{p}_0) \equiv \exp(i(\alpha_1(\mathbf{p}) + \alpha_1(\mathbf{p}_0))H) \overline{\mathbf{X}}_{s\epsilon_1, \epsilon_2}^{(n)}(\mathbf{p}|\mathbf{p}_0)$, and the subscripts ϵ_1, ϵ_2 in $\overline{\mathbf{X}}_{s\epsilon_1, \epsilon_2}$ means that we replace ϵ_0 by ϵ_1 , and ϵ_1 by ϵ_2 in (61-63).

C A slab with a rough surface on the upper side

We consider a slab delimited on the upper side by a two-dimensional rough surface, and on the bottom side by a planar surface, see Fig. 7. To derive the reduced Rayleigh equation for this configuration, we have to combine the two following equations :

$$\int \frac{d^2\mathbf{p}}{(2\pi)^2} \overline{M}_h^{1+,0+}(\mathbf{u}|\mathbf{p}) \cdot \overline{R}_u(\mathbf{p}|\mathbf{p}_0) \cdot \mathbf{E}^i(\mathbf{p}_0) + \overline{M}_h^{1+,0-}(\mathbf{u}|\mathbf{p}_0) \cdot \mathbf{E}^i(\mathbf{p}_0) = \frac{2(\epsilon_0 \epsilon_1)^{\frac{1}{2}} \alpha_1(\mathbf{u})}{(\epsilon_1 - \epsilon_0)} \mathbf{E}^{1+}(\mathbf{u}), \quad (100)$$

$$\int \frac{d^2\mathbf{p}}{(2\pi)^2} \overline{M}_h^{1-,0+}(\mathbf{u}|\mathbf{p}) \cdot \overline{R}_u(\mathbf{p}|\mathbf{p}_0) \cdot \mathbf{E}^i(\mathbf{p}_0) + \overline{M}_h^{1-,0-}(\mathbf{u}|\mathbf{p}_0) \cdot \mathbf{E}^i(\mathbf{p}_0) = -\frac{2(\epsilon_0 \epsilon_1)^{\frac{1}{2}} \alpha_1(\mathbf{u})}{(\epsilon_1 - \epsilon_0)} \mathbf{E}^{1-}(\mathbf{u}), \quad (101)$$

with

$$\mathbf{E}^{1+}(\mathbf{u}) = \overline{V}^{H21}(\mathbf{u}) \cdot \mathbf{E}^{1-}(\mathbf{u}), \quad (102)$$

where \overline{V}^{H21} is given by (86), and \overline{R}_u is the global scattering matrix for the upper rough surface and the bottom planar surface.

The reduced Rayleigh equation for the scattering matrix \overline{R}_u is then

$$\int \frac{d^2\mathbf{p}}{(2\pi)^2} \left[\overline{M}_h^{1+,0+}(\mathbf{u}|\mathbf{p}) + \overline{V}^{H21}(\mathbf{u}) \cdot \overline{M}_h^{1-,0+}(\mathbf{u}|\mathbf{p}) \right] \cdot \overline{R}_u(\mathbf{p}|\mathbf{p}_0) = - \left[\overline{M}_h^{1+,0-}(\mathbf{u}|\mathbf{p}_0) + \overline{V}^{H21}(\mathbf{u}) \cdot \overline{M}_h^{1-,0-}(\mathbf{u}|\mathbf{p}_0) \right]. \quad (103)$$

With the expansion of $I(\alpha|\mathbf{p})$ in power series, we obtain the perturbative development:

$$\begin{aligned} \overline{X}_u^{(0)}(\mathbf{p}_0) &= - \left[\frac{\overline{M}^{1+,0+}(\mathbf{p}_0|\mathbf{p}_0)}{\alpha_1(\mathbf{p}_0) - \alpha_0(\mathbf{p}_0)} - \overline{V}^{H21}(\mathbf{p}_0) \cdot \frac{\overline{M}^{1-,0+}(\mathbf{p}_0|\mathbf{p}_0)}{\alpha_1(\mathbf{p}_0) + \alpha_0(\mathbf{p}_0)} \right]^{-1} \\ &\quad \cdot \left[\frac{\overline{M}^{1+,0-}(\mathbf{p}_0|\mathbf{p}_0)}{\alpha_1(\mathbf{p}_0) + \alpha_0(\mathbf{p}_0)} + \overline{V}^{H21}(\mathbf{p}_0) \cdot \frac{\overline{M}^{1-,0-}(\mathbf{p}_0|\mathbf{p}_0)}{-\alpha_1(\mathbf{p}_0) + \alpha_0(\mathbf{p}_0)} \right] \\ &= \left(\overline{V}^{10}(\mathbf{p}_0) + \overline{V}^{H21}(\mathbf{p}_0) \right) \cdot \left[\overline{1} + \overline{V}^{10}(\mathbf{p}_0) \cdot \overline{V}^{H21}(\mathbf{p}_0) \right]^{-1}, \end{aligned} \quad (104)$$

$$\overline{X}_u^{(1)}(\mathbf{u}|\mathbf{p}_0) \equiv 2i \overline{Q}^{++}(\mathbf{u}|\mathbf{p}_0) \quad (105)$$

$$\overline{X}_u^{(2)}(\mathbf{u}|\mathbf{p}_1|\mathbf{p}_0) = \alpha_1(\mathbf{u}) \overline{Q}^{-+}(\mathbf{u}|\mathbf{p}_0) + \alpha_0(\mathbf{p}_0) \overline{Q}^{+-}(\mathbf{u}|\mathbf{p}_0) - 2 \overline{P}^+(\mathbf{u}|\mathbf{p}_1) \cdot \overline{Q}^{++}(\mathbf{p}_1|\mathbf{p}_0) \quad (106)$$

$$\begin{aligned} \overline{X}_u^{(3)}(\mathbf{u}|\mathbf{p}_1|\mathbf{p}_2|\mathbf{p}_0) &= -\frac{i}{3} \left[(\alpha_1^2(\mathbf{u}) + \alpha_0^2(\mathbf{p}_0)) \overline{Q}^{++}(\mathbf{u}|\mathbf{p}_0) + 2 \alpha_1(\mathbf{u}) \alpha_0(\mathbf{p}_0) \overline{Q}^{--}(\mathbf{u}|\mathbf{p}_0) \right] \\ &\quad + i \overline{P}^+(\mathbf{u}|\mathbf{p}_1) \cdot \overline{X}^{(2)}(\mathbf{p}_1|\mathbf{p}_2|\mathbf{p}_0) + i \left[\alpha_1(\mathbf{u}) \overline{P}^-(\mathbf{u}|\mathbf{p}_2) - \alpha_0(\mathbf{p}_2) \overline{P}^+(\mathbf{u}|\mathbf{p}_2) \right] \cdot \overline{Q}^{++}(\mathbf{p}_2|\mathbf{p}_0) \end{aligned} \quad (107)$$

with

$$\begin{aligned} \overline{Q}^{ba}(\mathbf{u}|\mathbf{p}_0) &\equiv \frac{1}{2 \alpha_0(\mathbf{p}_0)} \left[\frac{\overline{M}^{1+,0+}(\mathbf{u}|\mathbf{u})}{\alpha_1(\mathbf{u}) - \alpha_0(\mathbf{u})} - \overline{V}^{H21}(\mathbf{u}) \cdot \frac{\overline{M}^{1-,0+}(\mathbf{u}|\mathbf{u})}{\alpha_1(\mathbf{u}) + \alpha_0(\mathbf{u})} \right]^{-1} \\ &\quad \cdot \left[a \overline{M}^{1+,0+}(\mathbf{u}|\mathbf{p}_0) \cdot \overline{X}_{s\epsilon_0,\epsilon_1}^{(0)}(\mathbf{p}_0) + \overline{M}^{1+,0-}(\mathbf{u}|\mathbf{p}_0) \right. \\ &\quad \left. + b \overline{V}^{H21}(\mathbf{u}) \cdot \left(a \overline{M}^{1-,0+}(\mathbf{u}|\mathbf{p}_0) \cdot \overline{X}_{s\epsilon_0,\epsilon_1}^{(0)}(\mathbf{p}_0) + \overline{M}^{1-,0-}(\mathbf{u}|\mathbf{p}_0) \right) \right], \end{aligned} \quad (108)$$

$$\begin{aligned} \overline{P}^\pm(\mathbf{u}|\mathbf{p}_1) &\equiv \left[\frac{\overline{M}^{1+,0+}(\mathbf{u}|\mathbf{u})}{\alpha_1(\mathbf{u}) - \alpha_0(\mathbf{u})} - \overline{V}^{H21}(\mathbf{u}) \cdot \frac{\overline{M}^{1-,0+}(\mathbf{u}|\mathbf{u})}{\alpha_1(\mathbf{u}) + \alpha_0(\mathbf{u})} \right]^{-1} \\ &\quad \cdot \left[\overline{M}^{1+,0+}(\mathbf{u}|\mathbf{p}_1) \pm \overline{V}^{H21}(\mathbf{u}) \cdot \overline{M}^{1-,0+}(\mathbf{u}|\mathbf{p}_1) \right], \end{aligned} \quad (109)$$

where, $a = \pm$, $b = \pm$ are the sign indices. After some computations we obtain:

$$\begin{aligned} \overline{Q}^{++}(\mathbf{u}|\mathbf{p}_0) &= (\epsilon_1 - \epsilon_0) [\overline{D}_{10}^+(\mathbf{u})]^{-1} \cdot \\ &\begin{pmatrix} \epsilon_1 \|\mathbf{u}\| \|\mathbf{p}_0\| F_V^+(\mathbf{u}) F_V^+(\mathbf{p}_0) & -\epsilon_0^{\frac{1}{2}} K_0 \alpha_1(\mathbf{u}) F_V^-(\mathbf{u}) F_H^+(\mathbf{p}_0) (\hat{\mathbf{u}} \times \hat{\mathbf{p}}_0)_z \\ -\epsilon_0 \alpha_1(\mathbf{u}) \alpha_1(\mathbf{p}_0) F_V^-(\mathbf{u}) F_V^-(\mathbf{p}_0) \hat{\mathbf{u}} \cdot \hat{\mathbf{p}}_0 & \\ -\epsilon_0^{\frac{1}{2}} K_0 \alpha_1(\mathbf{p}_0) F_H^+(\mathbf{u}) F_V^-(\mathbf{p}_0) (\hat{\mathbf{u}} \times \hat{\mathbf{p}}_0)_z & K_0^2 F_H^+(\mathbf{u}) F_H^+(\mathbf{p}_0) \hat{\mathbf{u}} \cdot \hat{\mathbf{p}}_0 \end{pmatrix} \cdot [\overline{D}_{10}^+(\mathbf{p}_0)]^{-1}, \end{aligned} \quad (110)$$

$$\begin{aligned} \overline{Q}^{-+}(\mathbf{u}|\mathbf{p}_0) &= (\epsilon_1 - \epsilon_0) [\overline{D}_{10}^+(\mathbf{u})]^{-1} \cdot \\ &\begin{pmatrix} \epsilon_1 \|\mathbf{u}\| \|\mathbf{p}_0\| F_V^-(\mathbf{u}) F_V^+(\mathbf{p}_0) & -\epsilon_0^{\frac{1}{2}} K_0 \alpha_1(\mathbf{u}) F_V^+(\mathbf{u}) F_H^+(\mathbf{p}_0) (\hat{\mathbf{u}} \times \hat{\mathbf{p}}_0)_z \\ -\epsilon_0 \alpha_1(\mathbf{u}) \alpha_1(\mathbf{p}_0) F_V^+(\mathbf{u}) F_V^-(\mathbf{p}_0) \hat{\mathbf{u}} \cdot \hat{\mathbf{p}}_0 & \\ -\epsilon_0^{\frac{1}{2}} K_0 \alpha_1(\mathbf{p}_0) F_H^-(\mathbf{u}) F_V^-(\mathbf{p}_0) (\hat{\mathbf{u}} \times \hat{\mathbf{p}}_0)_z & K_0^2 F_H^-(\mathbf{u}) F_H^+(\mathbf{p}_0) \hat{\mathbf{u}} \cdot \hat{\mathbf{p}}_0 \end{pmatrix} \cdot [\overline{D}_{10}^+(\mathbf{p}_0)]^{-1}, \end{aligned} \quad (111)$$

$$\begin{aligned} \overline{Q}^{+-}(\mathbf{u}|\mathbf{p}_0) &= \frac{(\epsilon_1 - \epsilon_0)}{\alpha_0(\mathbf{p}_0)} [\overline{D}_{10}^+(\mathbf{u})]^{-1} \cdot \\ &\begin{pmatrix} \epsilon_0 \alpha_1(\mathbf{p}_0) \|\mathbf{u}\| \|\mathbf{p}_0\| F_V^+(\mathbf{u}) F_V^-(\mathbf{p}_0) & -\epsilon_0^{\frac{1}{2}} K_0 \alpha_1(\mathbf{u}) \alpha_1(\mathbf{p}_0) F_V^-(\mathbf{u}) F_H^-(\mathbf{p}_0) (\hat{\mathbf{u}} \times \hat{\mathbf{p}}_0)_z \\ -\epsilon_1 \alpha_1(\mathbf{u}) \alpha_0^2(\mathbf{p}_0) F_V^-(\mathbf{u}) F_V^+(\mathbf{p}_0) \hat{\mathbf{u}} \cdot \hat{\mathbf{p}}_0 & \\ -\epsilon_0^{-\frac{1}{2}} \epsilon_1 K_0 \alpha_0^2(\mathbf{p}_0) F_H^+(\mathbf{u}) F_V^+(\mathbf{p}_0) (\hat{\mathbf{u}} \times \hat{\mathbf{p}}_0)_z & K_0^2 \alpha_1(\mathbf{p}_0) F_H^+(\mathbf{u}) F_H^-(\mathbf{p}_0) \hat{\mathbf{u}} \cdot \hat{\mathbf{p}}_0 \end{pmatrix} \cdot [\overline{D}_{10}^+(\mathbf{p}_0)]^{-1}, \end{aligned} \quad (112)$$

$$\begin{aligned} \overline{Q}^{--}(\mathbf{u}|\mathbf{p}_0) &= \frac{(\epsilon_1 - \epsilon_0)}{\alpha_0(\mathbf{p}_0)} [\overline{D}_{10}^+(\mathbf{u})]^{-1} \cdot \\ &\begin{pmatrix} \epsilon_0 \alpha_1(\mathbf{p}_0) \|\mathbf{u}\| \|\mathbf{p}_0\| F_V^-(\mathbf{u}) F_V^-(\mathbf{p}_0) & -\epsilon_0^{\frac{1}{2}} K_0 \alpha_1(\mathbf{u}) \alpha_1(\mathbf{p}_0) F_V^+(\mathbf{u}) F_H^-(\mathbf{p}_0) (\hat{\mathbf{u}} \times \hat{\mathbf{p}}_0)_z \\ -\epsilon_1 \alpha_1(\mathbf{u}) \alpha_0^2(\mathbf{p}_0) F_V^+(\mathbf{u}) F_V^+(\mathbf{p}_0) \hat{\mathbf{u}} \cdot \hat{\mathbf{p}}_0 & \\ -\epsilon_0^{-\frac{1}{2}} \epsilon_1 K_0 \alpha_0^2(\mathbf{p}_0) F_H^-(\mathbf{u}) F_V^+(\mathbf{p}_0) (\hat{\mathbf{u}} \times \hat{\mathbf{p}}_0)_z & K_0^2 \alpha_1(\mathbf{p}_0) F_H^-(\mathbf{u}) F_H^-(\mathbf{p}_0) \hat{\mathbf{u}} \cdot \hat{\mathbf{p}}_0 \end{pmatrix} \cdot [\overline{D}_{10}^+(\mathbf{p}_0)]^{-1}, \end{aligned} \quad (113)$$

where

$$\begin{pmatrix} F_V^\pm(\mathbf{p}_0) & 0 \\ 0 & F_H^\pm(\mathbf{p}_0) \end{pmatrix} = \left(\overline{\mathbf{I}} \pm \overline{\mathbf{V}}^{H21}(\mathbf{p}_0) \right) \left[\overline{\mathbf{I}} + \overline{\mathbf{V}}^{10}(\mathbf{p}_0) \cdot \overline{\mathbf{V}}^{H21}(\mathbf{p}_0) \right]^{-1} \quad (114)$$

and

$$\overline{P}^+(\mathbf{u}|\mathbf{p}_1) = (\epsilon_1 - \epsilon_0) [\overline{D}_{10}^+(\mathbf{u})]^{-1} \cdot \begin{pmatrix} \|\mathbf{u}\| \|\mathbf{p}_1\| F_V^+(\mathbf{u}) & -\epsilon_0^{\frac{1}{2}} K_0 \alpha_1(\mathbf{u}) F_V^-(\mathbf{u}) (\hat{\mathbf{u}} \times \hat{\mathbf{p}}_1)_z \\ +\alpha_1(\mathbf{u}) \alpha_0(\mathbf{p}_1) F_V^-(\mathbf{u}) \hat{\mathbf{u}} \cdot \hat{\mathbf{p}}_1 & \\ \epsilon_0^{-\frac{1}{2}} K_0 \alpha_0(\mathbf{p}_1) F_H^+(\mathbf{u}) (\hat{\mathbf{u}} \times \hat{\mathbf{p}}_1)_z & K_0^2 F_H^+(\mathbf{u}) \hat{\mathbf{u}} \cdot \hat{\mathbf{p}}_1 \end{pmatrix}, \quad (115)$$

$$\overline{P}^-(\mathbf{u}|\mathbf{p}_1) = (\epsilon_1 - \epsilon_0) [\overline{D}_{10}^+(\mathbf{u})]^{-1} \cdot \begin{pmatrix} \|\mathbf{u}\| \|\mathbf{p}_1\| F_V^-(\mathbf{u}) & -\epsilon_0^{\frac{1}{2}} K_0 \alpha_1(\mathbf{u}) F_V^+(\mathbf{u}) (\hat{\mathbf{u}} \times \hat{\mathbf{p}}_1)_z \\ +\alpha_1(\mathbf{u}) \alpha_0(\mathbf{p}_1) F_V^+(\mathbf{u}) \hat{\mathbf{u}} \cdot \hat{\mathbf{p}}_1 & \\ \epsilon_0^{-\frac{1}{2}} K_0 \alpha_0(\mathbf{p}_1) F_H^-(\mathbf{u}) (\hat{\mathbf{u}} \times \hat{\mathbf{p}}_1)_z & K_0^2 F_H^-(\mathbf{u}) \hat{\mathbf{u}} \cdot \hat{\mathbf{p}}_1 \end{pmatrix}. \quad (116)$$

The first-order term was recently derived by Fuks *et al*¹⁴. They have noticed that for this order, the matrix differs from the one obtained for a surface separating two semi-infinite media by only the factors F^\pm . Likewise, for higher order, we see that Eqs. (110,111) differ from Eq. (66) by only F^\pm , similarly for Eqs. (112,113) with respect to Eq. (67), and Eqs. (115,116) with respect to Eq. (68). So when the thickness H becomes infinite, and the absorption $Im(\epsilon_1) \neq 0$, or if $\epsilon_1 = \epsilon_2$, we have $\overline{\mathbf{V}}^{H21} = 0$, thus $F^\pm = 1$, and in that case we recover the matrix (66-68) for a rough surface between two semi-infinite media.

V. THE MUELLER MATRIX CROSS SECTION AND THE SURFACE STATISTIC

When we consider an observation point in the far field limit, the saddle-point method gives an asymptotic form for the scattered field $\mathbf{E}^s \equiv \mathbf{E}^{0+}$ obtained from Eq. (51) :

$$\mathbf{E}^s(\mathbf{x}, z) = \frac{\exp(iK_0\|\mathbf{r}\|)}{\|\mathbf{r}\|} \overline{\mathbf{f}}(\mathbf{p}|\mathbf{p}_0) \cdot \mathbf{E}^i(\mathbf{p}_0), \quad (117)$$

with

$$\overline{\mathbf{f}}(\mathbf{p}|\mathbf{p}_0) \equiv \frac{K_0 \cos \theta}{2\pi i} \overline{\mathbf{R}}(\mathbf{p}|\mathbf{p}_0), \quad (118)$$

$$\mathbf{p} = K_0 \frac{\mathbf{x}}{\|\mathbf{r}\|}, \quad (119)$$

where θ is the angle between $\hat{\mathbf{e}}_z$ and the scattering direction (see Fig. 2). In order to describe the incident and the scattered waves, we introduce the modified Stokes parameters:

$$\mathbf{I}^s(\mathbf{p}) \equiv \begin{pmatrix} |E_V^s(\mathbf{p})|^2 \\ |E_H^s(\mathbf{p})|^2 \\ 2Re(E_V^s(\mathbf{p})E_H^s(\mathbf{p})) \\ 2Im(E_V^s(\mathbf{p})E_H^s(\mathbf{p})) \end{pmatrix}, \quad \mathbf{I}^i(\mathbf{p}_0) \equiv \begin{pmatrix} |E_V^i(\mathbf{p}_0)|^2 \\ |E_H^i(\mathbf{p}_0)|^2 \\ 2Re(E_V^i(\mathbf{p}_0)E_H^i(\mathbf{p}_0)) \\ 2Im(E_V^i(\mathbf{p}_0)E_H^i(\mathbf{p}_0)) \end{pmatrix}. \quad (120)$$

The analog of the scattering matrix for these parameters is the Mueller matrix, defined² by:

$$\mathbf{I}^s(\mathbf{p}) \equiv \frac{1}{\|\mathbf{r}\|^2} \overline{\mathbf{M}}(\mathbf{p}|\mathbf{p}_0) \cdot \mathbf{I}^i(\mathbf{p}_0), \quad (121)$$

which can be expressed as a function² of $\overline{\mathbf{f}}(\mathbf{p}|\mathbf{p}_0)$. To maintain a matrix formulation in the following calculations, we introduce a new product between two-dimensional matrices with the definition :

$$\begin{aligned} \overline{\mathbf{f}} \odot \overline{\mathbf{g}} &\equiv \begin{pmatrix} f_{VV} & f_{VH} \\ f_{HV} & f_{HH} \end{pmatrix} \odot \begin{pmatrix} g_{VV} & g_{VH} \\ g_{HV} & g_{HH} \end{pmatrix} \\ &= \begin{pmatrix} f_{VV}g_{VV}^* & f_{VH}g_{VH}^* & Re(f_{VV}g_{VH}^*) & -Im(f_{VV}g_{VH}^*) \\ f_{HV}g_{HV}^* & f_{HH}g_{HH}^* & Re(f_{HV}g_{HH}^*) & -Im(f_{HV}g_{HH}^*) \\ 2Re(f_{VV}g_{HV}^*) & 2Re(f_{VH}g_{HH}^*) & Re(f_{VV}g_{VV}^* + f_{HV}g_{VH}^*) & -Im(f_{VV}g_{HH}^* - f_{VH}g_{HV}^*) \\ 2Im(f_{VV}g_{HV}^*) & 2Im(f_{VH}g_{HH}^*) & Im(f_{VV}g_{VV}^* + f_{HV}g_{VH}^*) & Re(f_{VV}g_{HH}^* - f_{VH}g_{HV}^*) \end{pmatrix}. \end{aligned} \quad (122)$$

This product allows to express the matrix $\overline{\mathbf{M}}$ as :

$$\overline{\mathbf{M}}(\mathbf{p}|\mathbf{p}_0) = \overline{\mathbf{f}}(\mathbf{p}|\mathbf{p}_0) \odot \overline{\mathbf{f}}(\mathbf{p}|\mathbf{p}_0), \quad (123)$$

$$= \frac{K_0^2 \cos^2 \theta}{(2\pi)^2} \overline{\mathbf{R}}(\mathbf{p}|\mathbf{p}_0) \odot \overline{\mathbf{R}}(\mathbf{p}|\mathbf{p}_0). \quad (124)$$

Following Ishimaru *et al.*²⁸, we define the Mueller matrix cross section per unit area $\overline{\sigma} = (\sigma_{ij})$:

$$\overline{\sigma} \equiv \frac{4\pi}{A} \overline{\mathbf{M}}, \quad (125)$$

and, the bistatic Mueller matrix⁴ $\overline{\gamma} = (\gamma_{ij})$:

$$\overline{\gamma} \equiv \frac{1}{A \cos \theta_0} \overline{\mathbf{M}}. \quad (126)$$

These matrix are the generalization of the classical coefficients. In fact, if we assume, for example, that the incident wave is vertically polarized we have:

$$\frac{1}{A \cos \theta_0} |E_V^s(\mathbf{p})|^2 = \frac{1}{\|r\|^2} \gamma_{11}(\mathbf{p}|\mathbf{p}_0) |E_V^i(\mathbf{p})|^2, \quad (127)$$

$$\frac{1}{A \cos \theta_0} |E_H^s(\mathbf{p})|^2 = \frac{1}{\|r\|^2} \gamma_{21}(\mathbf{p}|\mathbf{p}_0) |E_V^i(\mathbf{p})|^2. \quad (128)$$

Thus γ_{11} and γ_{21} , are respectively the classical bistatic coefficients γ_{VV} and γ_{HV} . We can also define the cross section and the bistatic coefficients for an incident circular polarization. As an example, taking the incident wave right circularly polarized, we have

$$\mathbf{I}^i(\mathbf{p}_0) = \frac{1}{2} (1 \ 1 \ 0 \ -2)^t, \quad (129)$$

now, if we put a right-hand side polarizer at the receiver:

$$\frac{1}{4} \begin{pmatrix} 1 & 1 & 0 & 1 \\ 1 & 1 & 0 & 1 \\ 0 & 0 & 0 & 0 \\ 2 & 2 & 0 & 2 \end{pmatrix}, \quad (130)$$

the right to right bistatic coefficient γ_{rr} is:

$$\gamma_{rr} = \frac{1}{4} (\gamma_{11} + \gamma_{12} + 2\gamma_{14} + \gamma_{21} + \gamma_{22} + 2\gamma_{24} + \gamma_{41} + \gamma_{42} + 2\gamma_{44}), \quad (131)$$

where γ_{ij} are coefficients of the matrix $\overline{\gamma} = (\gamma_{ij})$.

In a similar way we obtain the right to left bistatic coefficient:

$$\gamma_{lr} = \frac{1}{4} (\gamma_{11} + \gamma_{12} + 2\gamma_{14} + \gamma_{21} + \gamma_{22} + 2\gamma_{24} - \gamma_{41} - \gamma_{42} - 2\gamma_{44}). \quad (132)$$

Up to now, we have made no hypothesis on the nature of the rough surface. Let us introduce the statistical characteristics of the function $h(\mathbf{x})$. We suppose that it is a stationary, isotropic Gaussian random process defined by the moments

$$\langle h(\mathbf{x}) \rangle = 0, \quad (133)$$

$$\langle h(\mathbf{x}) h(\mathbf{x}') \rangle = W(\mathbf{x} - \mathbf{x}'), \quad (134)$$

where the angle brackets denote an average over the ensemble of realizations of the function $h(\mathbf{x})$. In this work we will use a Gaussian form for the surface-height correlation function $W(\mathbf{x})$:

$$W(\mathbf{x}) = \sigma^2 \exp(-\mathbf{x}^2/l^2), \quad (135)$$

where σ is the rms height of the surface, and l is the transverse correlation length. In momentum space we have:

$$\langle h(\mathbf{p}) \rangle = 0, \quad (136)$$

$$\langle h(\mathbf{p}) h(\mathbf{p}') \rangle = (2\pi)^2 \delta(\mathbf{p} + \mathbf{p}') W(\mathbf{p}), \quad (137)$$

with

$$W(\mathbf{p}) \equiv \int d^2\mathbf{x} W(\mathbf{x}) \exp(-i\mathbf{p} \cdot \mathbf{x}) \quad (138)$$

$$= \pi \sigma^2 l^2 \exp(-\mathbf{p}^2 l^2/4). \quad (139)$$

We are now able to define the bistatic coherent matrix

$$\bar{\gamma}^{coh} \equiv \frac{1}{A \cos \theta_0} \langle \bar{\mathbf{f}}(\mathbf{p}|\mathbf{p}_0) \rangle \odot \langle \bar{\mathbf{f}}(\mathbf{p}|\mathbf{p}_0) \rangle = \frac{K_0^2 \cos^2 \theta}{A (2\pi)^2 \cos \theta_0} \langle \bar{\mathbf{R}}(\mathbf{p}|\mathbf{p}_0) \rangle \odot \langle \bar{\mathbf{R}}(\mathbf{p}|\mathbf{p}_0) \rangle, \quad (140)$$

and the incoherent bistatic matrix

$$\begin{aligned} \bar{\gamma}^{incoh}(\mathbf{p}|\mathbf{p}_0) &\equiv \frac{1}{A \cos \theta_0} [\langle \bar{\mathbf{f}}(\mathbf{p}|\mathbf{p}_0) \odot \bar{\mathbf{f}}(\mathbf{p}|\mathbf{p}_0) \rangle - \langle \bar{\mathbf{f}}(\mathbf{p}|\mathbf{p}_0) \rangle \odot \langle \bar{\mathbf{f}}(\mathbf{p}|\mathbf{p}_0) \rangle], \\ &= \frac{K_0^2 \cos^2 \theta}{A (2\pi)^2 \cos \theta_0} [\langle \bar{\mathbf{R}}(\mathbf{p}|\mathbf{p}_0) \odot \bar{\mathbf{R}}(\mathbf{p}|\mathbf{p}_0) \rangle - \langle \bar{\mathbf{R}}(\mathbf{p}|\mathbf{p}_0) \rangle \odot \langle \bar{\mathbf{R}}(\mathbf{p}|\mathbf{p}_0) \rangle]. \end{aligned} \quad (141)$$

From Eq. (53), and the property of the Gaussian random process, we obtain

$$\bar{\gamma}^{coh}(\mathbf{p}|\mathbf{p}_0) = \frac{K_0^2 \cos^2 \theta}{\cos \theta_0} \delta(\mathbf{p} - \mathbf{p}_0) \bar{\mathbf{R}}^{coh}(\mathbf{p}_0) \odot \bar{\mathbf{R}}^{coh}(\mathbf{p}_0) \quad (142)$$

$$\bar{\mathbf{R}}^{coh}(\mathbf{p}_0) \equiv \bar{\mathbf{X}}^{(0)}(\mathbf{p}_0) + K_0 \cos \theta_0 \int \frac{d^2 \mathbf{p}}{(2\pi)^2} \bar{\mathbf{X}}^{(2)}(\mathbf{p}_0|\mathbf{p}_1|\mathbf{p}_0) W(\mathbf{p}_1 - \mathbf{p}_0) + \dots, \quad (143)$$

where $\bar{\mathbf{R}}^{coh}(\mathbf{p}_0)$ is a diagonal matrix describing the reflection coefficients of the coherent waves. For the incoherent part we have :

$$\bar{\gamma}^{incoh}(\mathbf{p}|\mathbf{p}_0) = \frac{K_0^4 \cos^2 \theta \cos \theta_0}{(2\pi)^2} [\bar{\mathbf{I}}^{(1-1)}(\mathbf{p}|\mathbf{p}_0) + \bar{\mathbf{I}}^{(2-2)}(\mathbf{p}|\mathbf{p}_0) + \bar{\mathbf{I}}^{(3-1)}(\mathbf{p}|\mathbf{p}_0)], \quad (144)$$

where

$$\bar{\mathbf{I}}^{(1-1)}(\mathbf{p}|\mathbf{p}_0) \equiv W(\mathbf{p} - \mathbf{p}_0) \bar{\mathbf{X}}^{(1)}(\mathbf{p}|\mathbf{p}_0) \odot \bar{\mathbf{X}}^{(1)}(\mathbf{p}|\mathbf{p}_0) \quad (145)$$

$$\bar{\mathbf{I}}^{(2-2)}(\mathbf{p}|\mathbf{p}_0) \equiv \int \frac{d^2 \mathbf{p}_1}{(2\pi)^2} W(\mathbf{p} - \mathbf{p}_1) W(\mathbf{p}_1 - \mathbf{p}_0) \bar{\mathbf{X}}^{(2)}(\mathbf{p}|\mathbf{p}_1|\mathbf{p}_0) \odot [\bar{\mathbf{X}}^{(2)}(\mathbf{p}|\mathbf{p}_1|\mathbf{p}_0) + \bar{\mathbf{X}}^{(2)}(\mathbf{p}|\mathbf{p} + \mathbf{p}_0 - \mathbf{p}_1|\mathbf{p}_0)] \quad (146)$$

$$\bar{\mathbf{I}}^{(3-1)}(\mathbf{p}|\mathbf{p}_0) \equiv W(\mathbf{p} - \mathbf{p}_0) [\bar{\mathbf{X}}^{(1)}(\mathbf{p}|\mathbf{p}_0) \odot \bar{\mathbf{X}}^{(3)}(\mathbf{p}|\mathbf{p}_0) + \bar{\mathbf{X}}^{(3)}(\mathbf{p}|\mathbf{p}_0) \odot \bar{\mathbf{X}}^{(1)}(\mathbf{p}|\mathbf{p}_0)], \quad (147)$$

with

$$\begin{aligned} \bar{\mathbf{X}}^{(3)}(\mathbf{p}|\mathbf{p}_0) &\equiv \int \frac{d^2 \mathbf{p}_1}{(2\pi)^2} [W(\mathbf{p}_1 - \mathbf{p}_0) \bar{\mathbf{X}}^{(3)}(\mathbf{p}|\mathbf{p}_0|\mathbf{p}_1|\mathbf{p}_0) \\ &\quad + W(\mathbf{p} - \mathbf{p}_1) (\bar{\mathbf{X}}^{(3)}(\mathbf{p}|\mathbf{p}_1|\mathbf{p}_0 - \mathbf{p} + \mathbf{p}_1|\mathbf{p}_0) + \bar{\mathbf{X}}^{(3)}(\mathbf{p}|\mathbf{p}_1|\mathbf{p}|\mathbf{p}_0))] . \end{aligned} \quad (148)$$

VI. APPLICATIONS

In the previous sections we have developed a method to compute the scattering matrices for a rough surface between two media, and for a thin film which includes one rough surface. In this section, we will evaluate numerically the incoherent bistatic coefficients given by (144-147) for different values of the parameters which characterize the configurations. In all numerical simulations the media 0 will be the vacuum ($\epsilon_0 = 1$).

A rough surface separating to different media

We consider that a polarized light of wavelength $\lambda = 457.9 \text{ nm}$ is normally incident ($\theta_0 = 0^\circ$, $\phi_0 = 0^\circ$) on a two-dimensional rough silver surface (see Fig. 3) characterized by the roughness parameters $\sigma = 5 \text{ nm}$, $l = 100 \text{ nm}$, $\epsilon = -7.5 + i0.24$. As a matter of comparison we have chosen the same parameters used for the scattering by a one-dimensional rough surface²¹. The perturbative development is given by Eqs. (61,68). In Fig. 8, we present the results for an incident wave linearly polarized, the scattered field being observed in the incident plane ($\phi = 0^\circ$). The single scattering contribution associated with the term $\bar{\mathbf{I}}^{(1-1)}$ is

plotted as a dotted line, the double-scattering contribution $\overline{\mathbf{T}}^{(2-2)}$ as a dashed line, the scattering term $\overline{\mathbf{T}}^{(3-1)}$ as a dash-dotted line, and the sum of all these terms $\overline{\mathbf{\gamma}}^{incoh}$ by the solid curve.

We observed an enhancement of the backscattering which corresponds to the physical process in which the incident light excites a surface electromagnetic wave. In fact, the surface polariton propagates along the rough surface, then it is scattered into a volume wave due to the roughness, at the same time, a reverse partner exists with a path travelling in the opposite direction. These two paths can interfere constructively near the backscattering direction to produce a peak^{17,18,19}. However, in one dimension²¹, this peak can only be observed for a (TM) polarized incident wave because a surface polariton only exists for this polarization. In two dimensions, the surface wave also exists for a (TM) polarization, but in fact a depolarization occurs so that a (TE) incident wave can excite a (TM) surface wave, and this surface wave can be scattered into volume wave with both polarizations as can be seen in Fig. 8. Now, when the incident wave is circularly polarized, we see in Fig. 9, that the enhanced backscattering takes also place. We have not displayed the left to left, and left to right polarizations because the media are not optically active, as a consequence, the results are the same either the incident wave is right or left polarized.

In the expression (144), the peak is produced by the term $\overline{\mathbf{T}}^{(2-2)}$. We see that the term $\overline{\mathbf{P}}(\mathbf{u}|\mathbf{p}_1) \cdot \overline{\mathbf{Q}}^+(\mathbf{p}_1|\mathbf{p}_0)$ in $\overline{\mathbf{X}}_{s\epsilon_0,\epsilon_1}^{(2)}(\mathbf{p}|\mathbf{p}_1|\mathbf{p}_0)$ contains a factor of the form (see Eq. (58)):

$$[D_{10V}^+(\mathbf{p}_1)]^{-1} = \frac{1}{\epsilon_1\alpha_0(\mathbf{p}_1) + \epsilon_0\alpha_1(\mathbf{p}_1)}, \quad (149)$$

which is close to zero excepted when \mathbf{p}_1 is near the resonance mode \mathbf{p}_r of the polariton, which is given by the roots $D_{10V}^+(\mathbf{p}_r) = 0$. When we observe the field scattered far away from the backscattering direction ($\mathbf{p} + \mathbf{p}_0 \neq 0$), the terms $\overline{\mathbf{X}}_{s\epsilon_0,\epsilon_1}^{(2)}(\mathbf{p}|\mathbf{p}_1|\mathbf{p}_0)$ and $\overline{\mathbf{X}}_{s\epsilon_0,\epsilon_1}^{(2)}(\mathbf{p}|\mathbf{p} + \mathbf{p}_0 - \mathbf{p}_1|\mathbf{p}_0)$ containing D_{10V}^+ are non zero when $\mathbf{p}_1 \approx \mathbf{p}_r$, and $\mathbf{p} + \mathbf{p}_0 - \mathbf{p}_1 \approx \mathbf{p}_r$ respectively. Since these domains are disjoint, the product \odot of these two terms is approximatively zero. Conversely, when we are near the backscattering direction ($\mathbf{p} + \mathbf{p}_0 \approx 0$), the terms inside brackets are almost equal and produce the enhancement factor. This enhancement factor is not equal to 2 because the matrices $\overline{\mathbf{Q}}^+(\mathbf{p}|\mathbf{p}_0)$ and $\overline{\mathbf{Q}}^-(\mathbf{p}|\mathbf{p}_0)$ in $\overline{\mathbf{X}}_{s\epsilon_0,\epsilon_1}^{(2)}$ do not contain the term $[D_{10V}^+(\mathbf{p}_1)]^{-1}$, so they produce a significative contribution whatever the scattering angle is. In order to isolate more precisely the terms producing an enhanced backscattering, a better approach is to work with the formalism of Ref. 16 derived from quantum mechanical scattering theory, such an approach is used for instance in Ref. 17,23. If the decomposition of each step of the mutiple scattering process is clearly put in evidence, however, it offers the disadvantage to produce a more heavier perturbative development as it can be seen when comparing (53) and (66-68) with (15-19,A-1) of Ref. 22.

A film with a rough surface on the upper side

We consider a dielectric film (see Fig. 7) of mean thickness $H = 500 \text{ nm}$, dielectric constant $\epsilon_1 = 2.6896 + 0.0075i$, deposited on a planar perfectly conducting substrate ($\epsilon_2 = -\infty$) and illuminated by a linearly polarized light of wavelength $\lambda = 632.8 \text{ nm}$ normally incident ($\phi_0 = 0^\circ$, $\theta_0 = 0^\circ$). The two-dimensional upper rough surface is characterized by the parameters $\sigma = 15 \text{ nm}$ and $l = 100 \text{ nm}$. The scattering diagrams are shown in Fig. 10 with the same curve labelling as before. The perturbative development being given by Eqs. (105,107) and Eqs. (110,116). Since we have chosen an infinite conducting plane ($\epsilon_2 = -\infty$) the coefficients F^\pm (Eq. (114)) have the following form :

$$F_V^\pm(\mathbf{p}_0) = \frac{1 \pm \exp(2i\alpha_0(\mathbf{p}_0)H)}{(\epsilon_1\alpha_0(\mathbf{p}_0) + \epsilon_0\alpha_1(\mathbf{p}_0)) + (\epsilon_1\alpha_0(\mathbf{p}_0) - \epsilon_0\alpha_1(\mathbf{p}_0)) \exp(2i\alpha_0(\mathbf{p}_0)H)}, \quad (150)$$

$$F_H^\pm(\mathbf{p}_0) = \frac{1 \mp \exp(2i\alpha_0(\mathbf{p}_0)H)}{(\alpha_0(\mathbf{p}_0) + \alpha_1(\mathbf{p}_0)) + (\alpha_0(\mathbf{p}_0) - \alpha_1(\mathbf{p}_0)) \exp(2i\alpha_0(\mathbf{p}_0)H)}. \quad (151)$$

The parameters are the same as those used in Ref. 23 for a one-dimensional dielectric film where a (TE) polarized wave is incident. The thickness was chosen in way that the slab supports only two guided wave modes, $p_{TE}^1 = 1.5466 K_0$, and $p_{TE}^2 = 1.2423 K_0$ for the (TE) polarization. These modes are resonance modes, they verify $[F_H^\pm]^{-1}(p_{TE}^{1,2}) = 0$. For the (TM) case, we have three modes given by the roots $[F_V^\pm]^{-1}(p_{TM}) = 0$, which are : $p_{TM}^1 = 1.6126 K_0$, $p_{TM}^2 = 1.3823 K_0$ and $p_{TM}^3 = 1.0030 K_0$. As described in Ref. 11,23,27, these guided modes can produce a classical enhanced backscattering with satellite peaks symmetrically positioned. The satellite peaks angles are given by the equation :

$$\sin \theta_\pm^{nm} = -\sin \theta_0 \pm \frac{1}{K_0} [p^n - p^m], \quad (152)$$

where p^n, p^m describe one of the guided mode, when $n = m$, we recover the classical enhanced backscattering. We can give an explanation of this formula as in the previous case. In the expression (106), the term producing the peaks comes from

$$-2\overline{\mathbf{P}}(\mathbf{u}|\mathbf{p}_1) \cdot \overline{\mathbf{Q}}^+(\mathbf{p}_1|\mathbf{p}_0) \quad (153)$$

where $\overline{\mathbf{Q}}^+(\mathbf{p}_1|\mathbf{p}_0)$ contains the factors $F^\pm(\mathbf{p}_1)$ having resonances for the slab guided mode. The product

$$\overline{\mathbf{X}}_d^{(2)}(\mathbf{p}|\mathbf{p}_1|\mathbf{p}_0) \odot \overline{\mathbf{X}}_d^{(2)}(\mathbf{p}|\mathbf{p} + \mathbf{p}_0 - \mathbf{p}_1|\mathbf{p}_0) \quad (154)$$

in Eq. (146) has a significant contribution only when \mathbf{p}_1 and $\mathbf{p} + \mathbf{p}_0 - \mathbf{p}_1$ are near resonance modes. As there are several resonances, we can have $\mathbf{p}_1 \approx \mathbf{p}_n$ and $\mathbf{p} + \mathbf{p}_0 - \mathbf{p}_1 \approx \mathbf{p}_m$ with $n \neq m$ where \mathbf{p}_n and \mathbf{p}_m are resonances vector. If $\mathbf{p}_n = \pm p_n \hat{e}_x$ and $\mathbf{p}_m = \mp p_m \hat{e}_x$ (guided modes propagating along the incident plane but with opposite directions), we have $(\mathbf{p} + \mathbf{p}_0) \cdot \hat{e}_x \approx \pm(p_n - p_m)$ which is another way of writing Eq. (152). For the (TE) polarization, since we have only two guided waves, the satellite peaks can only exist at the angles $\theta_\pm^{12}(TE) = \pm 17.7^\circ$. Now, for the (TM) polarization we have three possibilities: $\theta_\pm^{12}(TM) = \pm 13.3^\circ$, $\theta_\pm^{13}(TM) = \pm 37.6^\circ$, and $\theta_\pm^{23}(TM) = \pm 22.3^\circ$. The satellite peaks are produced by the term $\overline{\mathbf{I}}^{(2-2)}$, in the case of (TM) polarization we do not get any significant contribution to satellite peaks. However, for the (TE) to (TE) scattering shown in Fig. 11, we find satellite peaks at the angle $\theta_\pm^{12}(TE) = \pm 17.7^\circ$ positioned along a dotted line. Now, by doubling the slab thickness, see Fig. 12, the satellite peaks disappear for all the polarization, but we see a new phenomenon called the Selényi fringes.^{27,29,30} For a slightly random rough surface, the slab produces fringes similar to those obtain with a Fabry-Perrot interferometer illuminated by an extended source. The roughness modulates amplitude fringes but their localization remains the same as for the interferometer. We also notice that the enhanced backscattering decreases with the slab thickness. We can conclude that as in the case of one-dimensional rough surface, the satellite peaks appear only when the wave guide supports few modes for the (TE) polarizations. These results differ from those obtained in Ref. 27 where no satellite peak appears in their two-dimensional slab, we have checked that with their parameters values we also find no peak, and we agree with the results given by the contributions of the first and second order terms. However, the third order gives a contribution larger than the first one, such a result casts some doubt on the validity of the (SPM) method in that case.

However, for the choice of parameters presented here no satellite peak has been observed even when the thickness of the slab is chosen in such a way that only two guided modes exist for the (TM) polarization (a result not presented here). This is in agreement with the results of Ref. 31 for one dimensional surface where it is noticed that the excitation of (TM) modes are more difficult to excite than the (TE) modes. In order to enhance this effect they choose a higher permittivity for the media 1 : $\epsilon_1 = 5.6644 + i0.005$. In this case satellite peaks are observed for a slab which supports three guided modes. We have also done numerical calculations with these parameters, however we do not observe satellite peaks. So the transition from one dimensional to two dimensional rough surface lower the efficiency of the excitation of (TM) modes. Next, instead of doubling the slab thickness, we have changed the infinite conducting plane by a silver plane ($\epsilon_2 = -18.3 + 0.55i$), we see in Fig. 13, that the enhancement of backscattering is also decreased, and that there is no more satellite peak corresponding to (TE) to (TE) scattering. This fact has to be compared with the next configuration, where the rough surface is now between the media 1 and the media 2, see Fig. 4.

A film with a rough surface on the bottom side

The permittivities are the same as in the previous configuration, excepted that the case $\epsilon_2 = -\infty$ cannot be treated with the (SPM) because the second and third order diverge. The rms height σ has now the value $\sigma = 5 \text{ nm}$ and $l = 100 \text{ nm}$. We have not chosen $\sigma = 15 \text{ nm}$ because numerically we have noticed that the first order term $\overline{\mathbf{I}}^{(1-1)}$ was not greater than the second order $\overline{\mathbf{I}}^{(2-2)}$, which means that we are near the limit of validity of (SPM). The perturbative development is given by (97-99), and the guided modes are the roots of $[X_{VVd}^{(0)}(p_{TM})]^{-1}$ for (TM) polarization, and of $[X_{HHd}^{(0)}(p_{TE})]^{-1}$ for (TE) polarization. We obtain two modes in the (TE) case, whose values are : $p_{TE}^1 = 1.5534 K_0$, and $p_{TE}^2 = 1.2727 K_0$, the corresponding satellite peaks angles are : $\theta_\pm^{12}(TE) = \pm 16.3^\circ$. For the (TM) case, we have three guided modes with $p_{TM}^1 = 1.7752 K_0$, $p_{TM}^2 = 1.4577 K_0$ and $p_{TM}^3 = 1.034 K_0$, they correspond to six possible satellite peaks angles given by $\theta_\pm^{12}(TM) = \pm 18.51^\circ$, $\theta_\pm^{13}(TM) = \pm 47.8^\circ$, and $\theta_\pm^{23}(TM) = \pm 25^\circ$. We see the apparition of satellite peaks only for (TM) to (TM) scattering process as shown in Fig. 14.

This result differs from the previous case because, on one hand, the rough surface being not a perfect conductor we still obtain satellite peaks, on the other hand, these satellite peaks now appear for the (TM) to (TM) polarization instead of (TE) to (TE) . This is a surprising result because the (TM) polarization which has one more mode than the (TE) one, should decrease the amplitude of the satellite peaks for this polarization as it was the case with an upper rough boundary. Moreover, we see in Fig. 15, that the three satellite peaks can be clearly separated. This can be explained from the fact that there are two phenomenons which occur in this case. The first is the same as in the previous case where the wave can excite guided modes through the roughness which produces the enhancement of backscattering and the satellite peaks. These effects come from the term

$$\alpha_1(\mathbf{p}_1) \overline{\mathbf{X}}_{s \epsilon_1, \epsilon_2}^{H(1)}(\mathbf{p}|\mathbf{p}_1) \cdot \overline{\mathbf{U}}^{(0)}(\mathbf{p}_1) \cdot \overline{\mathbf{V}}^{10}(\mathbf{p}_1) \cdot \overline{\mathbf{X}}_{s \epsilon_1, \epsilon_2}^{H(1)}(\mathbf{p}_1|\mathbf{p}_0) \quad (155)$$

in Eq. (98) where $\overline{\mathbf{U}}^{(0)}(\mathbf{p}_1)$ have resonances for the different modes of the guided wave. But, there is also a second phenomenon which was described in our first example where the rough surface can excite a plasmon mode. This appears from Eq. (98) with the term

$$\overline{\mathbf{X}}_{s \epsilon_1, \epsilon_2}^{H(2)}(\mathbf{p}|\mathbf{p}_1|\mathbf{p}_0) \quad (156)$$

and subsequently in Eqs. (144,146). The localization of this mode \mathbf{p}_r is given by :

$$[D_{21}^+{}_{VV}(\mathbf{p}_r)]^{-1} = \frac{1}{\epsilon_2 \alpha_1(\mathbf{p}_r) + \epsilon_1 \alpha_2(\mathbf{p}_r)}. \quad (157)$$

In our case this give $\|\mathbf{p}_r\| = 1.7755 K_0$ which is very close to the value $p_{TM}^1 = 1.7752 K_0$. So, in Eq. (146) the product \odot of (155) by (156) can produce peaks where $\mathbf{p}_1 = \pm \|\mathbf{p}_r\| \hat{\mathbf{e}}_x \approx \pm p_{TM}^1 \hat{\mathbf{e}}_x$ and $(\mathbf{p}_0 + \mathbf{p}) \cdot \hat{\mathbf{e}}_x = \pm (p_{TM}^1 - p_{TM}^n)$ with $n = 1, 2, 3$. We have effectively verified numerically that the product of this two term can enhanced considerably the different peaks in particular the first satellite peaks θ_{\pm}^{12} (when $n = 2$). Now, by doubling the slab thickness, we see from Fig. 16 that the satellite peaks have disappeared due to the too many guided modes which can be excited.

VII. CONCLUSIONS

We have obtained four generalized reduced Rayleigh equations which are exact integral equations, and where one of the four unknown fields coming on the rough surface has been eliminated. These equations offer a systematic method to compute the small perturbation development without lengthy calculations, moreover, the scattering matrices are only two dimensional. All the theoretical calculations have been done up to order three in the height elevation which allow us to obtain all the fourth-order cross-section terms. We have calculated the perturbative development for three different structures composed of a rough surface separating to semi-infinite media, and a dielectric film where one of the two boundaries is a rough surface. For the first structure, the perturbative expression has been already calculated at the third order, but our derivation offers the advantage to be formulated in compact manner making easier numerical computations. For the slabs configuration we present new results. It has to be noticed that for the case of a rough surface in the upper position, the generalized derivation of the reduced Rayleigh equations becomes mandatory. The numerical results show an enhancement of the backscattering for co- and cross-polarizations in all these cases. In the slab case, for some configurations and definite polarizations, we have detected satellite peaks which result from interference of different waveguide modes. This general formulation can be extended to the configuration including two rough surfaces, and some results will be presented in a next paper.

ACKNOWLEDGMENTS

(AS) thanks ANRT for financial support during the preparation of his thesis (contract CIFRE-238-98).

APPENDIX A: THE INTEGRATION BY PARTS

We need to calculate the following integral:

$$\int d^2\mathbf{x} \exp(-i(\mathbf{k}_u^{1b} - \mathbf{k}_p^{1a}) \cdot \mathbf{r}_x) \nabla h(\mathbf{x}). \quad (\text{A1})$$

Since $\nabla h(x, y)$ is zero for $|x| > L/2$ or $|y| > L/2$, we can fix the integration limits. We choose the boundary limits x_l in x such that $|x_l| > L/2$, and $(\mathbf{u} - \mathbf{p})_x x_l = 2\pi m_x$, with $m_x \in \mathbb{Z}$. Similarly, we choose the boundary y_l in y such that $|y_l| > L/2$ and $(\mathbf{u} - \mathbf{p})_y y_l = 2\pi m_y$, with $m_y \in \mathbb{Z}$. Thus, the integral (A1) is :

$$\begin{aligned} & \int_{-x_l}^{x_l} \int_{-y_l}^{y_l} dx dy \exp(-i(\mathbf{u} - \mathbf{p}) \cdot \mathbf{x}) \nabla h(\mathbf{x}) \exp(-i(b\alpha_1(\mathbf{u}) - a\alpha_1(\mathbf{p}))h(\mathbf{x})) \\ &= \hat{\mathbf{e}}_x \int_{-y_l}^{y_l} dy \left[\frac{\exp(-i(\mathbf{u} - \mathbf{p}) \cdot \mathbf{x} - i(b\alpha_1(\mathbf{u}) - a\alpha_1(\mathbf{p}))h(\mathbf{x}))}{-i(b\alpha_1(\mathbf{u}) - a\alpha_1(\mathbf{p}))} \right]_{x=-x_l}^{x=+x_l} \\ &+ \hat{\mathbf{e}}_y \int_{-x_l}^{x_l} dx \left[\frac{\exp(-i(\mathbf{u} - \mathbf{p}) \cdot \mathbf{x} - i(b\alpha_1(\mathbf{u}) - a\alpha_1(\mathbf{p}))h(\mathbf{x}))}{-i(b\alpha_1(\mathbf{u}) - a\alpha_1(\mathbf{p}))} \right]_{y=-y_l}^{y=+y_l} \\ &- \int_{-x_l}^{x_l} \int_{-y_l}^{y_l} \frac{-i(\mathbf{u} - \mathbf{p})}{-i(b\alpha_1(\mathbf{u}) - a\alpha_1(\mathbf{p}))} \exp(-i(\mathbf{u} - \mathbf{p}) \cdot \mathbf{x} - i(b\alpha_1(\mathbf{u}) - a\alpha_1(\mathbf{p}))h(\mathbf{x})) \end{aligned} \quad (\text{A2})$$

$$= - \int d^2\mathbf{x} \frac{(\mathbf{u} - \mathbf{p})}{(b\alpha_1(\mathbf{u}) - a\alpha_1(\mathbf{p}))} \exp(-i(\mathbf{k}_u^{1b} - \mathbf{k}_p^{1a}) \cdot \mathbf{r}_x). \quad (\text{A3})$$

The term in the square bracket canceled due to the choice made for x_l and y_l . From the previous calculations, we can now replace $\nabla h(\mathbf{x})$ by:

$$\nabla h(\mathbf{x}) \longleftrightarrow - \frac{(\mathbf{u} - \mathbf{p})}{(b\alpha_1(\mathbf{u}) - a\alpha_1(\mathbf{p}))}. \quad (\text{A4})$$

APPENDIX B: PERTURBATIVE DEVELOPMENT AND RECIPROCITY CONDITION

As was noticed by Voronovich,⁸ the scattering operator $\bar{\mathbf{R}}$ has a very simple law of transformation when we shift the boundary in the horizontal direction by a vector \mathbf{d} :

$$\bar{\mathbf{R}}_{\mathbf{x} \rightarrow h(\mathbf{x}-\mathbf{d})}(\mathbf{p}|\mathbf{p}_0) = \exp[-i(\mathbf{p} - \mathbf{p}_0) \cdot \mathbf{d}] \bar{\mathbf{R}}_{\mathbf{x} \rightarrow h(\mathbf{x})}(\mathbf{p}|\mathbf{p}_0), \quad (\text{B1})$$

or, when we translate the surface by a vertical shift $H \hat{\mathbf{e}}_z$:

$$\bar{\mathbf{R}}_{h+H}(\mathbf{p}|\mathbf{p}_0) = \exp[-i(\alpha_0(\mathbf{p}) + \alpha_0(\mathbf{p}_0))H] \bar{\mathbf{R}}_h(\mathbf{p}|\mathbf{p}_0) \quad (\text{B2})$$

Now, using (B1), we can deduce some properties on the perturbative development of the scattering operator. The generalization of the Taylor expansion for a function depending on a real variable to an expansion depending on a function (which is in fact a fonctionnal) can be expressed in the following form:

$$\bar{\mathbf{R}}(\mathbf{p}|\mathbf{p}_0) = \bar{\mathbf{R}}^{(0)}(\mathbf{p}|\mathbf{p}_0) + \bar{\mathbf{R}}^{(1)}(\mathbf{p}|\mathbf{p}_0) + \bar{\mathbf{R}}^{(2)}(\mathbf{p}|\mathbf{p}_0) + \bar{\mathbf{R}}^{(3)}(\mathbf{p}|\mathbf{p}_0) + \dots, \quad (\text{B3})$$

where

$$\bar{\mathbf{R}}^{(1)}(\mathbf{p}|\mathbf{p}_0) = \int \frac{d^2\mathbf{p}_1}{(2\pi)^2} \bar{\mathbf{R}}^{(1)}(\mathbf{p}|\mathbf{p}_1|\mathbf{p}_0) h(\mathbf{p}_1), \quad (\text{B4})$$

$$\bar{\mathbf{R}}^{(2)}(\mathbf{p}|\mathbf{p}_0) = \iint \frac{d^2\mathbf{p}_1}{(2\pi)^2} \frac{d^2\mathbf{p}_2}{(2\pi)^2} \bar{\mathbf{R}}^{(2)}(\mathbf{p}|\mathbf{p}_1|\mathbf{p}_2|\mathbf{p}_0) h(\mathbf{p}_1) h(\mathbf{p}_2), \quad (\text{B5})$$

$$\bar{\mathbf{R}}^{(3)}(\mathbf{p}|\mathbf{p}_0) = \iiint \frac{d^2\mathbf{p}_1}{(2\pi)^2} \frac{d^2\mathbf{p}_2}{(2\pi)^2} \frac{d^2\mathbf{p}_3}{(2\pi)^2} \bar{\mathbf{R}}^{(3)}(\mathbf{p}|\mathbf{p}_1|\mathbf{p}_2|\mathbf{p}_3|\mathbf{p}_0) h(\mathbf{p}_1) h(\mathbf{p}_2) h(\mathbf{p}_3). \quad (\text{B6})$$

⋮

Applying this perturbative development on each side of (B1), and taking their functional derivative (see Ref. 7) defined by:

$$\frac{\delta^{(n)}}{\delta h(\mathbf{q}_1) \dots \delta h(\mathbf{q}_n)}. \quad (\text{B7})$$

We obtain for all $n \geq 0$ in the limit $h = 0$:

$$\overline{\mathbf{R}}^{(n)}(\mathbf{p}|\mathbf{q}_1|\dots|\mathbf{q}_n|\mathbf{p}_0) = \exp(-i(\mathbf{p} - \mathbf{q}_1 \dots - \mathbf{q}_n - \mathbf{p}_0) \cdot \mathbf{d}) \overline{\mathbf{R}}^{(n)}(\mathbf{p}|\mathbf{q}_1|\dots|\mathbf{q}_n|\mathbf{p}_0). \quad (\text{B8})$$

We find that

$$\overline{\mathbf{R}}^{(n)}(\mathbf{p}|\mathbf{q}_1|\dots|\mathbf{q}_n|\mathbf{p}_0) \propto \delta(\mathbf{p} - \mathbf{q}_1 \dots - \mathbf{q}_n - \mathbf{p}_0) \quad (\text{B9})$$

so we can define $\overline{\mathbf{X}}$ matrices by the relations :

$$\overline{\mathbf{R}}^{(0)}(\mathbf{p}|\mathbf{p}_0) = (2\pi)^2 \delta(\mathbf{p} - \mathbf{p}_0) \overline{\mathbf{X}}^{(0)}(\mathbf{p}_0), \quad (\text{B10})$$

$$\overline{\mathbf{R}}^{(1)}(\mathbf{p}|\mathbf{p}_0) = \alpha_0(\mathbf{p}_0) \overline{\mathbf{X}}^{(1)}(\mathbf{p}|\mathbf{p}_0) h(\mathbf{p} - \mathbf{p}_0), \quad (\text{B11})$$

$$\overline{\mathbf{R}}^{(2)}(\mathbf{p}|\mathbf{p}_0) = \alpha_0(\mathbf{p}_0) \int \frac{d^2 \mathbf{p}_1}{(2\pi)^2} \overline{\mathbf{X}}^{(2)}(\mathbf{p}|\mathbf{p}_1|\mathbf{p}_0) h(\mathbf{p} - \mathbf{p}_1) h(\mathbf{p}_1 - \mathbf{p}_0), \quad (\text{B12})$$

$$\overline{\mathbf{R}}^{(3)}(\mathbf{p}|\mathbf{p}_0) = \alpha_0(\mathbf{p}_0) \iint \frac{d^2 \mathbf{p}_1}{(2\pi)^2} \frac{d^2 \mathbf{p}_2}{(2\pi)^2} \overline{\mathbf{X}}^{(3)}(\mathbf{p}|\mathbf{p}_1|\mathbf{p}_2|\mathbf{p}_0) h(\mathbf{p} - \mathbf{p}_1) h(\mathbf{p}_1 - \mathbf{p}_2) h(\mathbf{p}_2 - \mathbf{p}_0), \quad (\text{B13})$$

⋮

where $\alpha_0(\mathbf{p}_0)$ is introduced for a matter of convenience.

Let us now make some remarks about the reciprocity condition. If we define the anti-transpose operation by:

$$\begin{pmatrix} a & b \\ c & d \end{pmatrix}^{aT} = \begin{pmatrix} a & -c \\ -b & d \end{pmatrix}, \quad (\text{B14})$$

the reciprocity condition for an incident and a scattered waves in the medium 0 reads⁸:

$$\frac{\overline{\mathbf{R}}^{aT}(\mathbf{p}|\mathbf{p}_0)}{\alpha_0(\mathbf{p}_0)} = \frac{\overline{\mathbf{R}}(-\mathbf{p}_0|-\mathbf{p})}{\alpha_0(\mathbf{p})}. \quad (\text{B15})$$

Making use of the previous functional derivative, we would like to prove that each order of the perturbative development must satisfies this condition. It is easy to show that

$$\left[\overline{\mathbf{X}}^{(1)}(\mathbf{p}|\mathbf{p}_0) \right]^{aT} = \overline{\mathbf{X}}^{(1)}(-\mathbf{p}_0|-\mathbf{p}), \quad (\text{B16})$$

thus $\overline{\mathbf{X}}^{(1)}$ is reciprocal, but the same conclusion cannot be extended to $\overline{\mathbf{X}}^{(n)}$ when $n \geq 2$. For example, in the case $n = 2$, using (B15), we can only deduce that:

$$\int \frac{d^2 \mathbf{p}_1}{(2\pi)^2} \left[\overline{\mathbf{X}}^{(2)}(\mathbf{p}|\mathbf{p}_1|\mathbf{p}_0) \right]^{aT} h(\mathbf{p} - \mathbf{p}_1) h(\mathbf{p}_1 - \mathbf{p}_0) = \int \frac{d^2 \mathbf{p}_1}{(2\pi)^2} \overline{\mathbf{X}}^{(2)}(-\mathbf{p}_0|-\mathbf{p}_1|-\mathbf{p}) h(\mathbf{p} - \mathbf{p}_1) h(\mathbf{p}_1 - \mathbf{p}_0). \quad (\text{B17})$$

From this we cannot deduce a result similar to (B16) for $\overline{\mathbf{X}}^{(2)}$. This fact is well illustrated with the following identity(which can be demonstrate with a transformation of the integration variables)) :

$$\int \frac{d^2 \mathbf{p}_1}{(2\pi)^2} (\mathbf{p} + \mathbf{p}_0 - 2\mathbf{p}_1) h(\mathbf{p} - \mathbf{p}_1) h(\mathbf{p}_1 - \mathbf{p}_0) = 0, \quad (\text{B18})$$

We see that $\mathbf{p}_1 \rightarrow \mathbf{p} + \mathbf{p}_0 - 2\mathbf{p}_1$ is not the null function although the integral is null. From this we deduce that $\overline{\mathbf{X}}^{(n)}$ for $n > 1$ are not unique. Moreover in using (B18) we can transform the $\overline{\mathbf{X}}^{(n)}$ in a reciprocal form. This procedure is illustrated in the one-dimensional case in Ref. 21, and the results for the second-order in the electromagnetic case are given in Ref. 8 and Ref. 22.

REFERENCES

- [†] Electronic address: soubret@cpt.univ-mrs.fr
- ¹ F.G. Bass and I.M. Fuks, *Wave Scattering from Statistically Rough Surfaces* (Pergamon, Oxford, U.K., 1979).
 - ² A. Ishimaru, *Wave Propagation and Scattering in Random Media* (Academic Press, New York, 1978).
 - ³ F.T. Ulaby, R.K. Moore, and A.K. Fung, *Microwave Remote Sensing* Vol. 2 (Addison-Wesley, Reading MA, 1986).
 - ⁴ L. Tsang, G.T.J. Kong, and R. Shin, *Theory of Microwave Remote Sensing* (Wiley-Interscience, New York, 1985).
 - ⁵ J.A. DeSanto and G.S. Brown, Progress in Optics XXIII, E. Wolf, ed, (Elsevier Science Publishers B. V. 1986).
 - ⁶ J.A. Ogilvy, *Theory of Wave Scattering From Random Rough Surfaces* (Adam Hilger, Bristol, 1991).
 - ⁷ S.M. Rytov, Y.A. Kravtsov and V.I. Tatarskii, *Principle of Statistical Radiophysics* (Springer-Verlag, vol. 3-4, 1989).
 - ⁸ A.G. Voronovich, *Wave Scattering from Rough Surfaces* (Springer, Berlin, 1994).
 - ⁹ A.K. Fung, *Microwave Scattering and Emission Models and their Applications* (Artech House, Boston-London, 1994).
 - ¹⁰ M. Nieto-Verperinas, *Scattering and Diffraction in Physical Optics* (Wiley, New-York, 1991)
 - ¹¹ V. Freilikher, E. Kanziiper, and A.A. Maradudin, Phys. Reports **288**, 127 (1997).
 - ¹² S.O. Rice, Comm. Pure Appl. Math. **4**, 351 (1951).
 - ¹³ J.T. Johnson, J. Opt. Soc. Am. A **16**, 2720 (1999). erratum J. Opt. Soc. Am. A **17**, 1685 (2000)
 - ¹⁴ I.M. Fuks and A.G. Voronovich, Waves in Random Media **10**, 253 (2000).
 - ¹⁵ A.G. Voronovich, Waves in Random Media **4**, 337 (1994).
 - ¹⁶ G.C. Brown, V. Celli, M. Haller, and A. Marvin, Surf. Sci. **136**, 381 (1984).
 - ¹⁷ A.R. McGurn, A.A. Maradudin, and V. Celli, Phys. Rev. B **31**, 4866 (1985).
 - ¹⁸ V. Celli, A.A. Maradudin, A.M. Marvin, and A.R. McGurn, J. Opt. Soc. Am. A **2**, 2225 (1985).
 - ¹⁹ A.R. McGurn and A.A. Maradudin, J. Opt. Soc. Am. B **4**, 910 (1987).
 - ²⁰ C. Baylard, J.J. Greffet, and A.A. Maradudin, J. Opt. Soc. Am. A **10**, 2637 (1993).
 - ²¹ A.A. Maradudin and E.R. Méndez, Appl. Opt. **32**, 3335 (1993).
 - ²² A.R. McGurn and A.A. Maradudin, Waves in Random Media **6**, 251 (1996).
 - ²³ J.A. Sánchez-Gil, A.A. Maradudin, J.Q. Lu, V.D. Freilikher, M. Pustilnik, and I. Yurkevich, Phys. Rev. B **50**, 15353 (1994).
 - ²⁴ J.J. Greffet, Phys. Rev. B **37**, 6436 (1988).
 - ²⁵ G. S. Brown, Wave Motion **7**, 195 (1985).
 - ²⁶ M. Nieto-Verperinas, J. Opt. Soc. Am. A **72**, 539 (1982).
 - ²⁷ T. Kawanishi, H. Ogura, and Z.L. Wang, Waves in Random Media **7**, 35 (1997).
 - ²⁸ A. Ishimaru, C. Le, Y. Kuga, L.A. Sengers, and T.K. Chan, PIER **14**, 1 (1996).
 - ²⁹ J.Q. Lu, J.A. Sánchez-Gil, E.R. Méndez, Z. Gu, and A.A. Maradudin, J. Opt. Soc. Am. A **15**, 185 (1998).
 - ³⁰ Y.S. Kaganovskii, V.D. Freilikher, E. Kanziiper, Y. Nafcha, M. Rosenbluh, and I.M. Fuks, J. Opt. Soc. Am. A **16**, 331 (1999).
 - ³¹ J.A. Sánchez-Gil, A.A. Maradudin, J.Q. Lu, V.D. Freilikher, M. Pustilnik, and I. Yurkevich, J. Mod. Opt. **43**, 435 (1996).
 - ³² However, we have to mention the work Ref. 27 where they consider a two-dimensional film. Their method has in principle the same domain of validity as the (SPM), the difference comes from their use of a sophisticated development called Wiener-Hermitte expansion to write down the scattered fields.
 - ³³ We use the same symbol for a function and its Fourier transform, they are differentiated by their arguments
 - ³⁴ We show explicitly the permittivity dependance of $\overline{\mathbf{R}}_s$ with the subscript ϵ_0, ϵ_1 because in the following section we will use the $\overline{\mathbf{R}}_s$ matrix with different permittivity values.
 - ³⁵ Throughout the paper, the symbol H in upper index is related to the height of a surface, in lower index to the polarization.

LIST OF FIGURES

1	A rough surface with an incident wave coming from both sides of medium 0 and 1.	24
2	Decomposition of the wave vector \mathbf{k}_p^{0+}	25
3	A two-dimensional rough surface separating two dielectric media 0 and 1.	26
4	A slab formed with a bottom two-dimensional rough surface and an upper planar surface.	27
5	Definitions of scattering matrices for a planar surface.	28
6	Diagrammatic representation of the operator $\bar{U}^{(0)}$	28
7	A slab formed with an upper two-dimensional rough surface and a bottom planar surface.	29
8	The bistatic coefficients for an horizontal (TE) and a vertical (TM) polarized incident light of wavelength $\lambda = 457.9 nm$ ($\theta_0 = 0^\circ$ and $\phi = \phi_0 = 0^\circ$), on a two-dimensional randomly rough silver surface, characterized by the parameters $\sigma = 5 nm$, $l = 100 nm$. $\epsilon_1 = -7.5 + i0.24$. For each figure are plotted : the total incoherent scattering $\bar{\gamma}^{incoh}$ (solid curve), the first order given by $\bar{T}^{(1-1)}$ (dotted line), the second order $\bar{T}^{(2-2)}$ (dashed line), and the third order $\bar{T}^{(3-1)}$ (dash-dotted line).	30
9	The same configuration as Fig. 8, but with a right incident circularly polarized wave, and a right to right (or left to left), right to left (or left to right) observed polarizations	31
10	The bistatic coefficients for an horizontal (TE) and a vertical (TM) polarized incident light of wavelength $\lambda = 632.8 nm$, on a slab with an upper two-dimensional randomly rough surface, characterized by the parameters $\sigma = 15 nm$, $l = 100 nm$, $\epsilon_1 = 2.6896 + i0.0075$, thickness $H = 500 nm$, deposited on an infinite conducting plane ($\epsilon_2 = -\infty$). The scattered field is observed in the incident plane. For each figure are plotted : the total incoherent scattering $\bar{\gamma}^{incoh}$ (solid curve), the first order given by $\bar{T}^{(1-1)}$ (dotted line), the second order $\bar{T}^{(2-2)}$ (dashed line), and the third order $\bar{T}^{(3-1)}$ (dash-dotted line).	32
11	Details of second order (TE) to (TE) contribution to the scattering shown in Fig. 10. We see two satellite peaks at the angle $\theta_{\pm}^{12}(TE) = \pm 17.7^\circ$, the dotted-lines mark the peaks angle position.	33
12	Effect of the slab thickness, $H = 1000 nm$, on the configuration shown in Fig. 10.	34
13	The same parameters as in Fig. 10, but with a silver plane characterized by $\epsilon_2 = -18.3 + 0.55i$.	35
14	The bistatic coefficients for an horizontal (TE) and vertical (TM) polarized light of wavelength $\lambda = 632.8 nm$, incident on a film of permittivity $\epsilon_1 = 2.6896 + i0.0075$, deposited on a two-dimensional randomly rough surface, characterized by the parameters, $\sigma = 5 nm$, $l = 100 nm$, $\epsilon_2 = -18.3 + 0.55i$, thickness $H = 500 nm$. The scattered field is observed in the incident plane. For each figure are plotted : the total incoherent scattering $\bar{\gamma}^{incoh}$ (solid curve), the first order given by $\bar{T}^{(1-1)}$ (dotted line), the second order $\bar{T}^{(2-2)}$ (dashed line), and the third order $\bar{T}^{(3-1)}$ (dash-dotted line).	36
15	Details of the second order (TM) to (TM) contribution to the scattering shown in Fig. 14, dotted lines mark the peaks angle position.	37
16	Effect of the slab thickness, $H = 1000 nm$, on the configuration shown in Fig. 14.	38

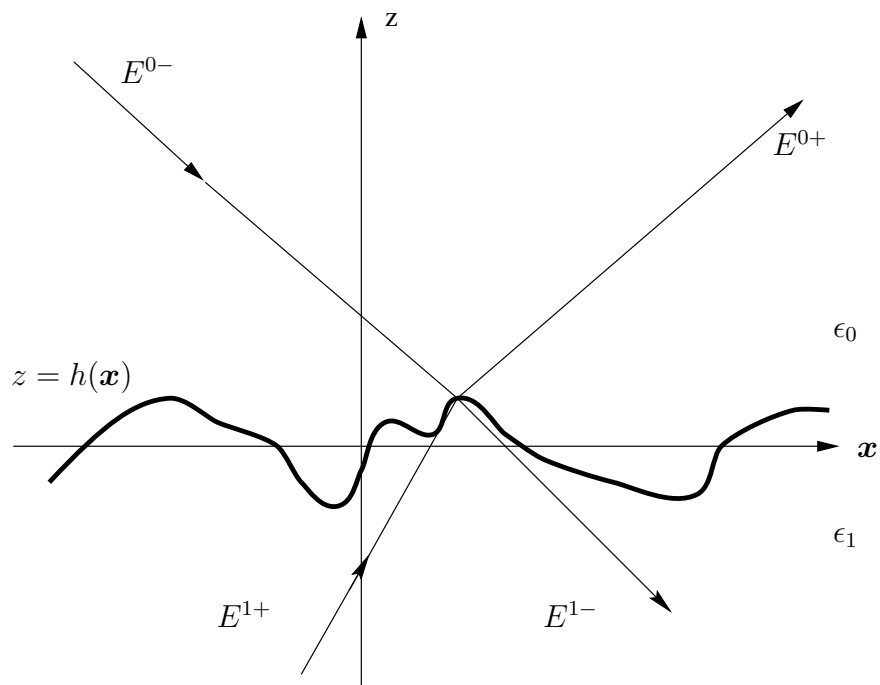


FIG. 1: A rough surface with an incident wave coming from both sides of medium 0 and 1.

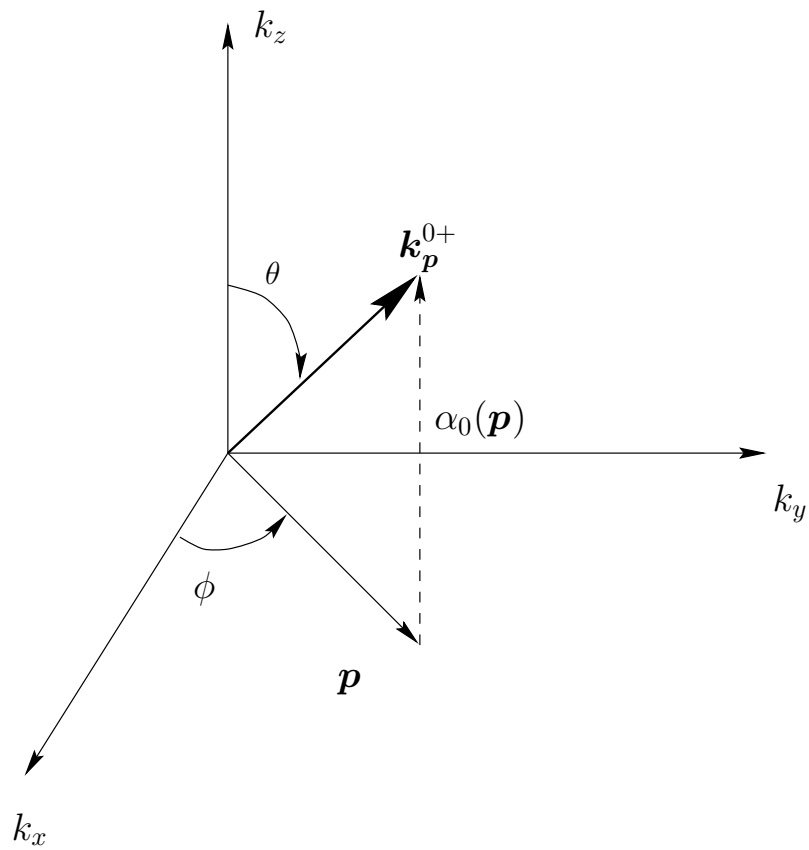


FIG. 2: Decomposition of the wave vector \mathbf{k}_p^{0+} .

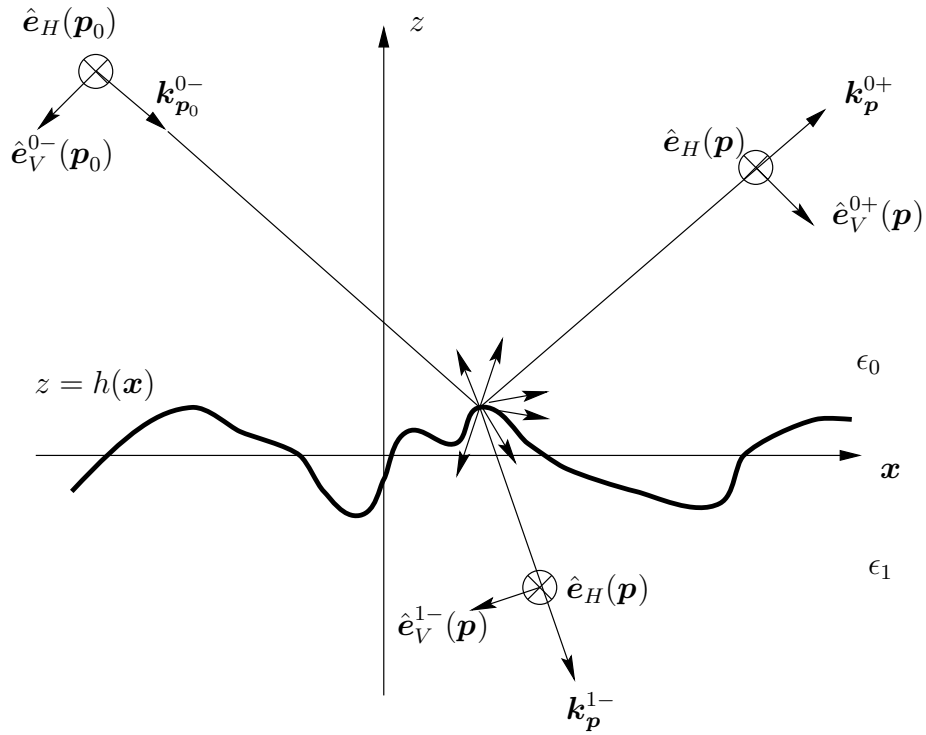


FIG. 3: A two-dimensional rough surface separating two dielectric media 0 and 1.

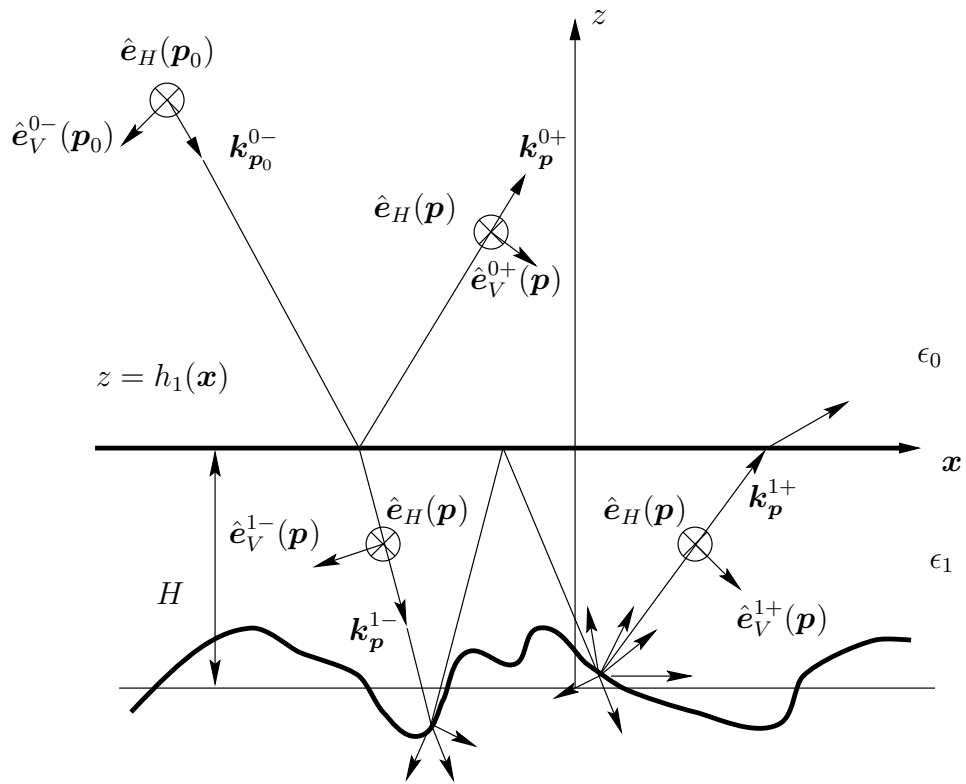


FIG. 4: A slab formed with a bottom two-dimensional rough surface and an upper planar surface.

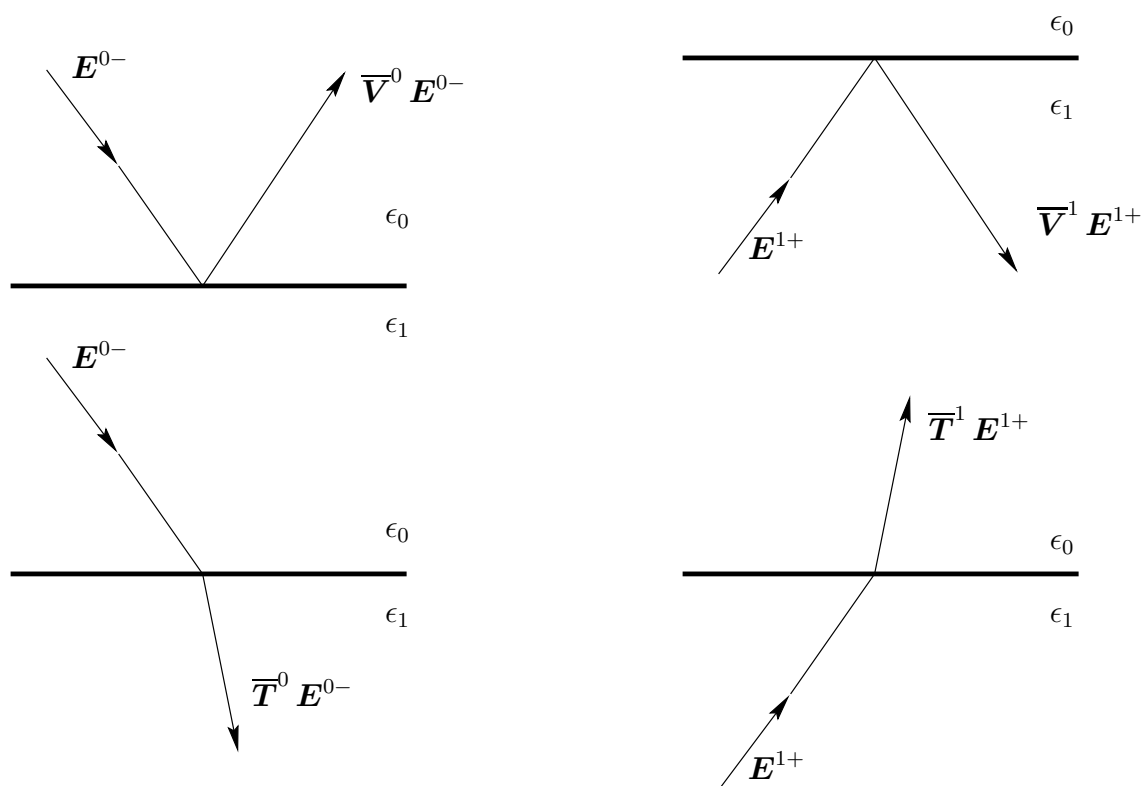


FIG. 5: Definitions of scattering matrices for a planar surface.

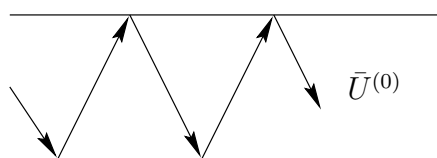


FIG. 6: Diagrammatic representation of the operator $\bar{U}^{(0)}$.

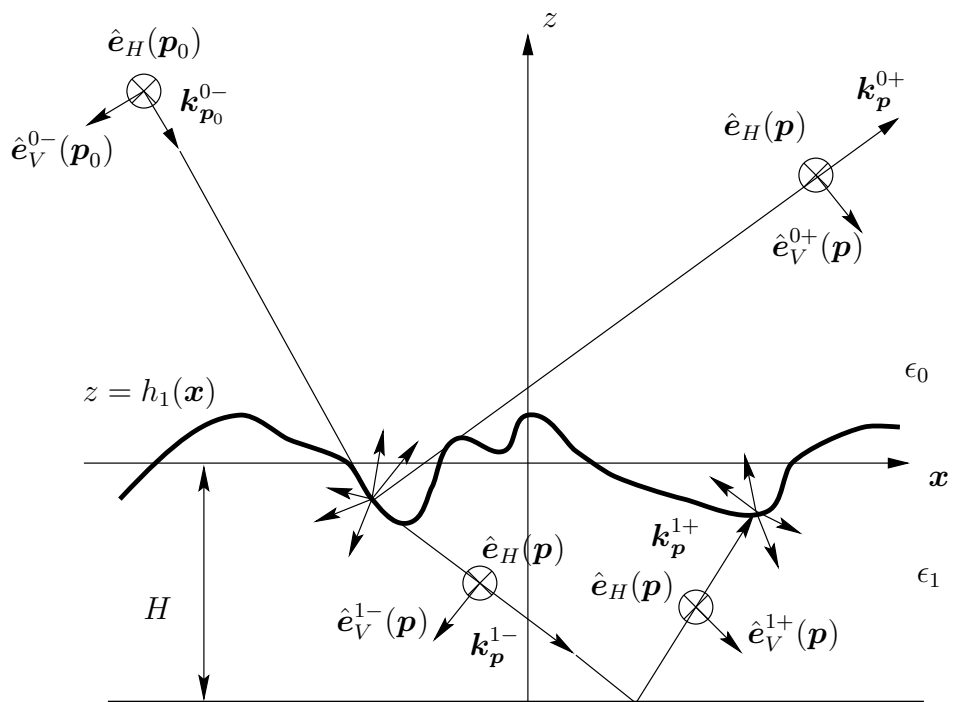


FIG. 7: A slab formed with an upper two-dimensional rough surface and a bottom planar surface.

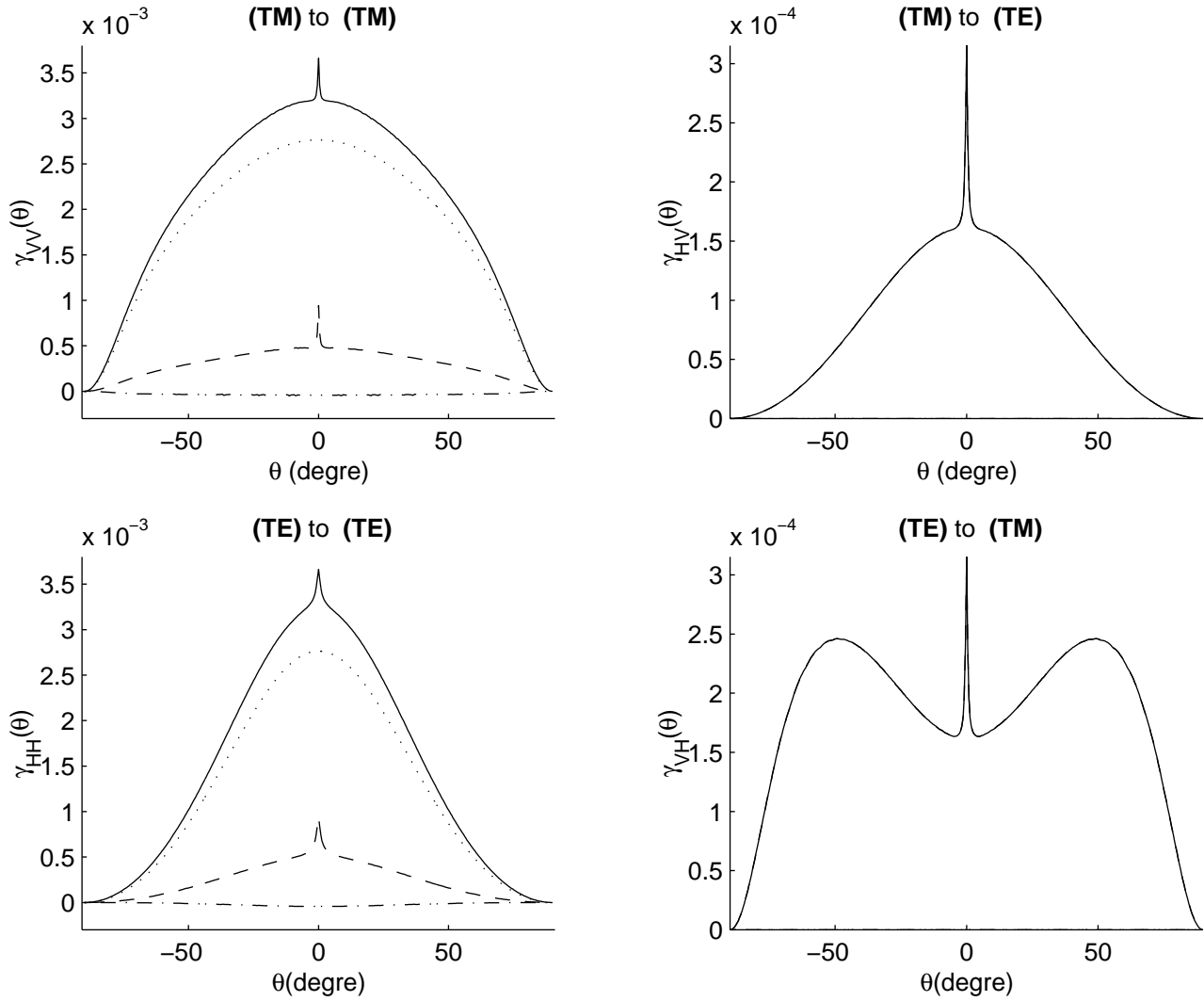


FIG. 8: The bistatic coefficients for an horizontal (*TE*) and a vertical (*TM*) polarized incident light of wavelength $\lambda = 457.9 \text{ nm}$ ($\theta_0 = 0^\circ$ and $\phi = \phi_0 = 0^\circ$), on a two-dimensional randomly rough silver surface, characterized by the parameters $\sigma = 5 \text{ nm}$, $l = 100 \text{ nm}$. $\epsilon_1 = -7.5 + i0.24$. For each figure are plotted : the total incoherent scattering $\bar{\gamma}^{incoh}$ (solid curve), the first order given by $\bar{\mathbf{I}}^{(1-1)}$ (dotted line), the second order $\bar{\mathbf{I}}^{(2-2)}$ (dashed line), and the third order $\bar{\mathbf{I}}^{(3-1)}$ (dash-dotted line).

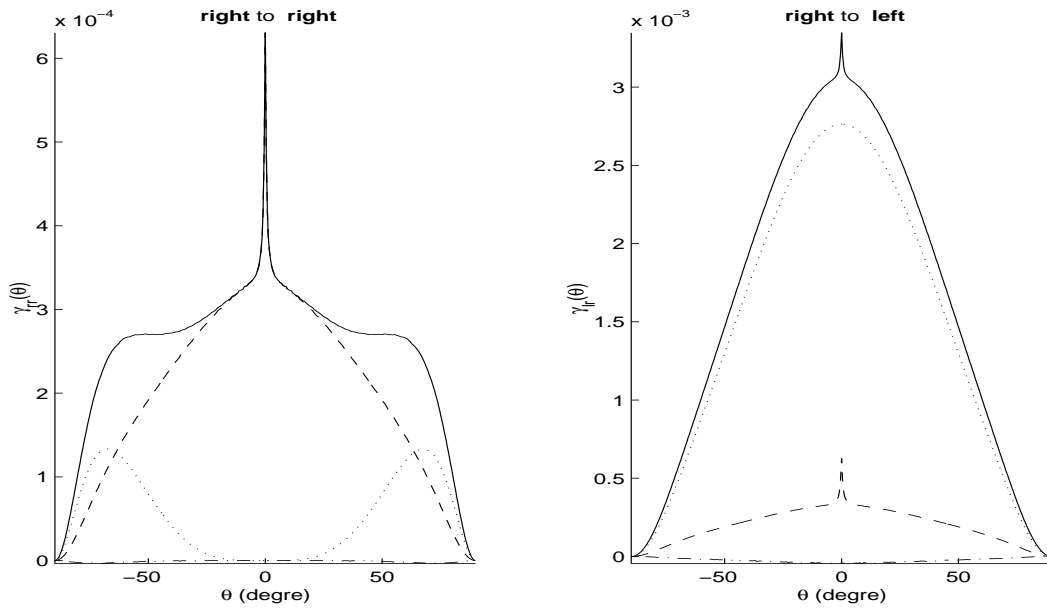


FIG. 9: The same configuration as Fig. 8, but with a right incident circularly polarized wave, and a right to right (or left to left), right to left (or left to right) observed polarizations

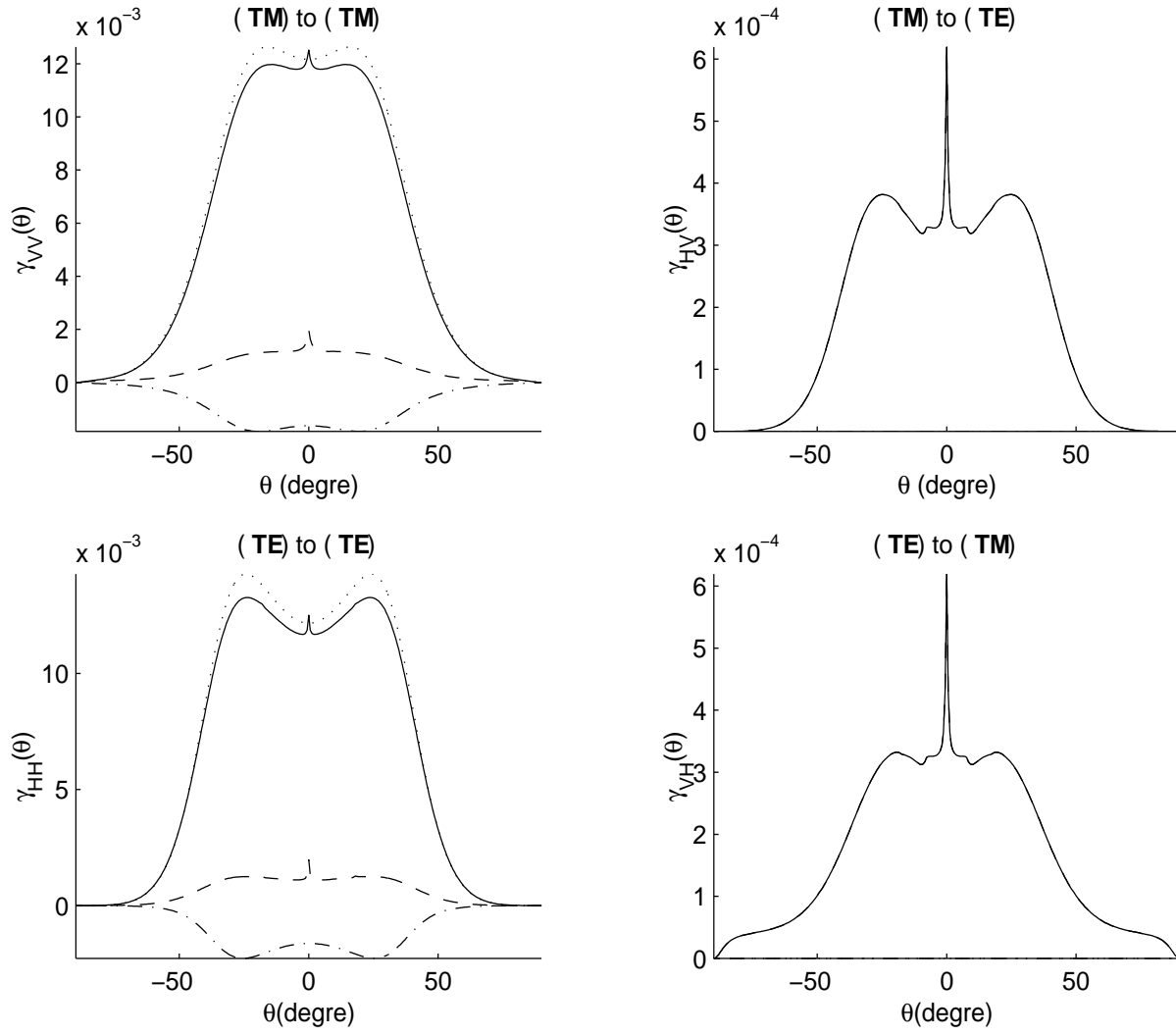


FIG. 10: The bistatic coefficients for an horizontal (*TE*) and a vertical (*TM*) polarized incident light of wavelength $\lambda = 632.8 \text{ nm}$, on a slab with an upper two-dimensional randomly rough surface, characterized by the parameters $\sigma = 15 \text{ nm}$, $l = 100 \text{ nm}$, $\epsilon_1 = 2.6896 + i0.0075$, thickness $H = 500 \text{ nm}$, deposited on an infinite conducting plane ($\epsilon_2 = -\infty$). The scattered field is observed in the incident plane. For each figure are plotted : the total incoherent scattering $\bar{\gamma}^{incoh}$ (solid curve), the first order given by $\bar{\mathbf{I}}^{(1-1)}$ (dotted line), the second order $\bar{\mathbf{I}}^{(2-2)}$ (dashed line), and the third order $\bar{\mathbf{I}}^{(3-1)}$ (dash-dotted line).

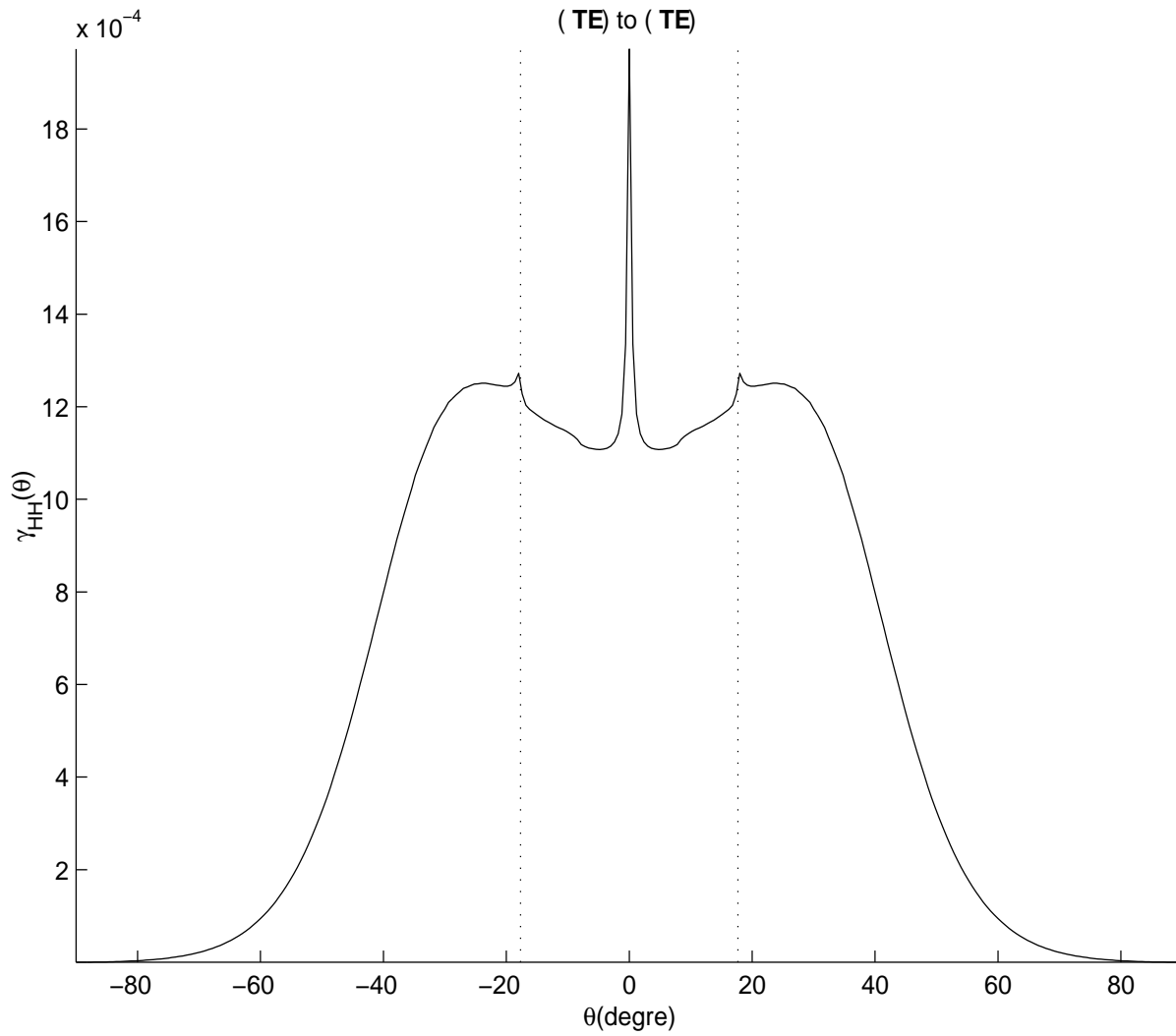


FIG. 11: Details of second order (TE) to (TE) contribution to the scattering shown in Fig. 10. We see two satellite peaks at the angle $\theta_{\pm}^{12}(TE) = \pm 17.7^\circ$, the dotted-lines mark the peaks angle position.

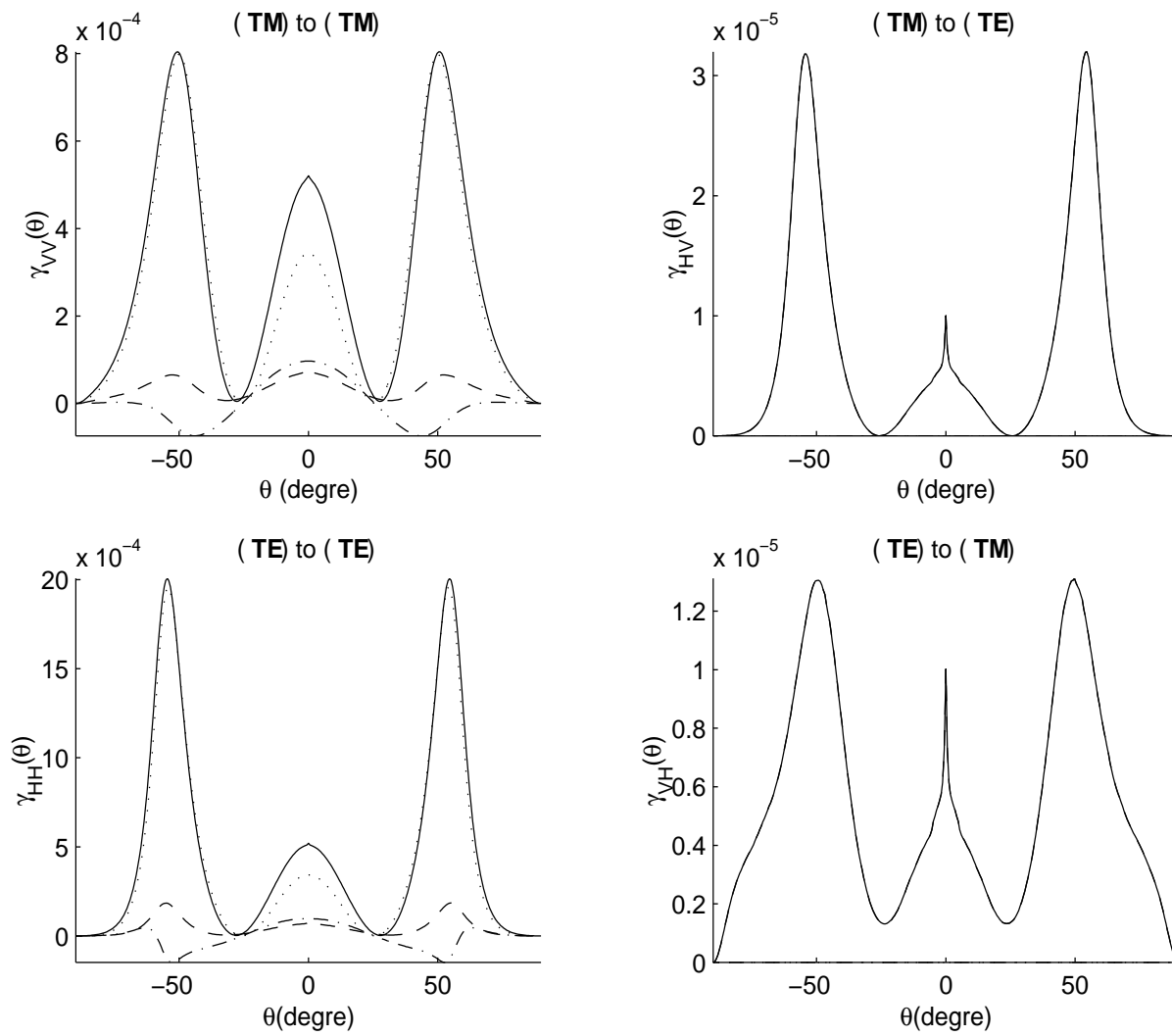


FIG. 12: Effect of the slab thickness, $H = 1000 \text{ nm}$, on the configuration shown in Fig. 10.

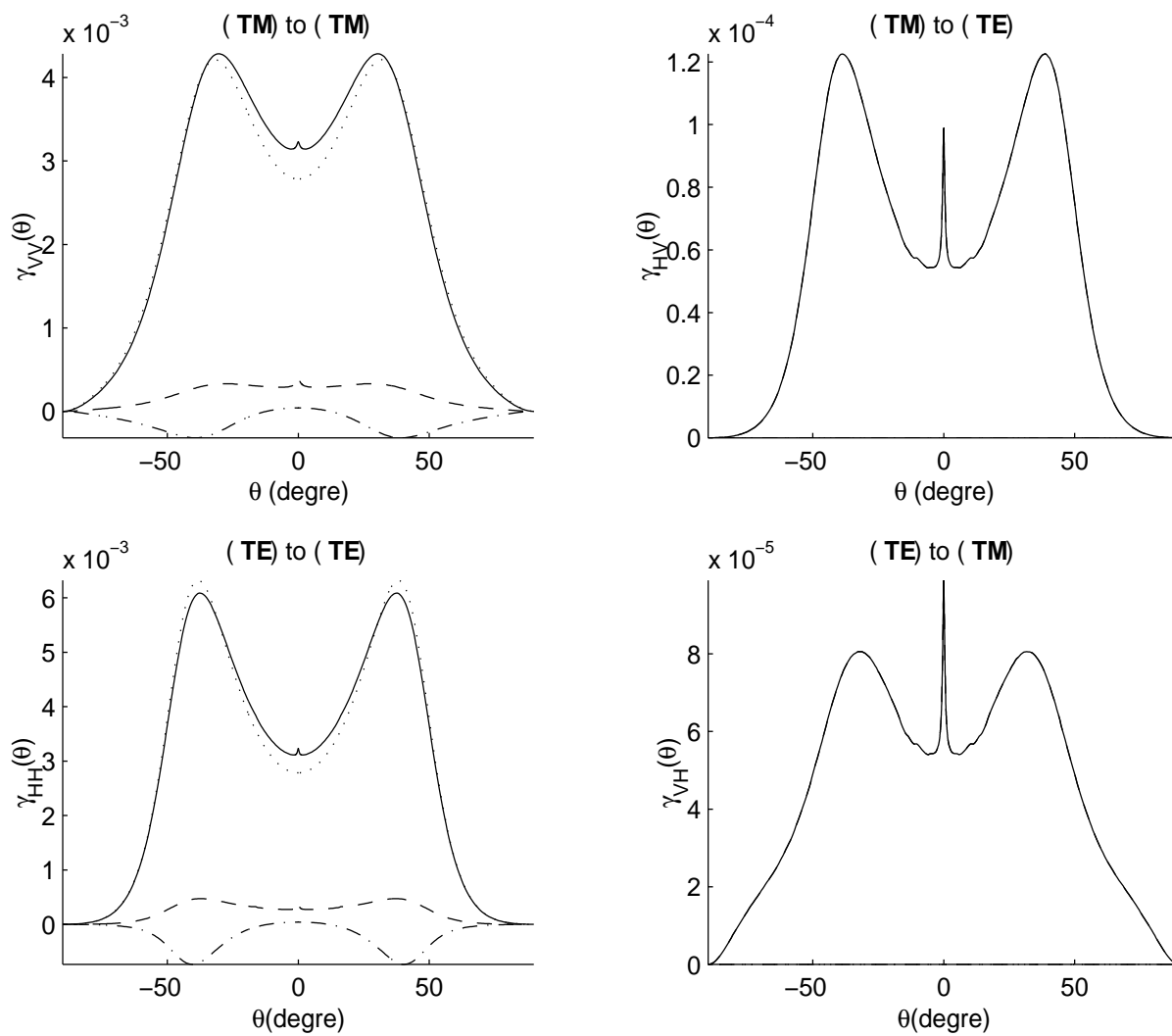


FIG. 13: The same parameters as in Fig. 10, but with a silver plane characterized by $\epsilon_2 = -18.3 + 0.55i$.

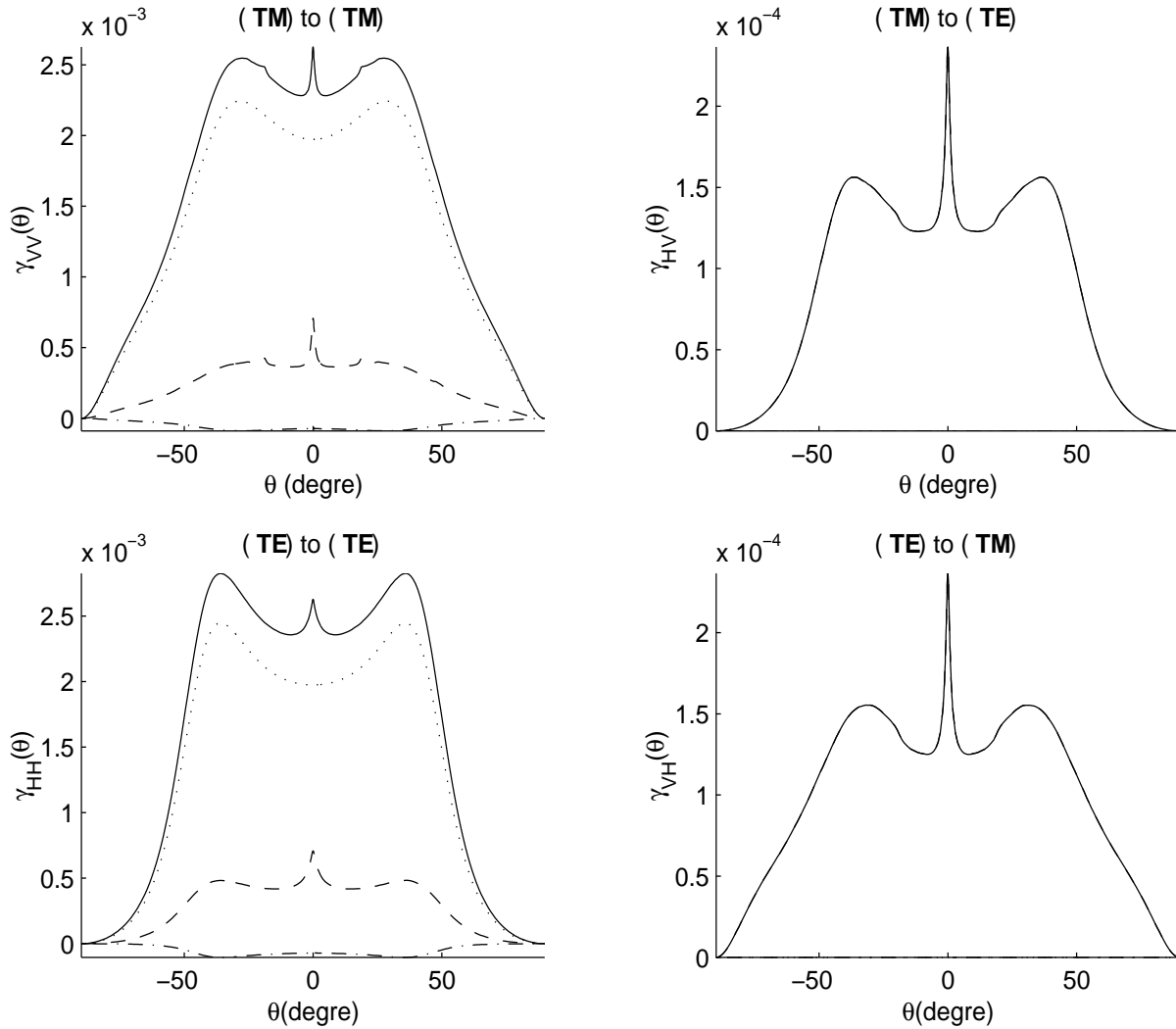


FIG. 14: The bistatic coefficients for an horizontal (*TE*) and vertical (*TM*) polarized light of wavelength $\lambda = 632.8 \text{ nm}$, incident on a film of permittivity $\epsilon_1 = 2.6896 + i0.0075$, deposited on a two-dimensional randomly rough surface, characterized by the parameters, $\sigma = 5 \text{ nm}$, $l = 100 \text{ nm}$, $\epsilon_2 = -18.3 + 0.55i$, thickness $H = 500 \text{ nm}$. The scattered field is observed in the incident plane. For each figure are plotted : the total incoherent scattering $\bar{\gamma}^{incoh}$ (solid curve), the first order given by $\bar{\mathbf{I}}^{(1-1)}$ (dotted line), the second order $\bar{\mathbf{I}}^{(2-2)}$ (dashed line), and the third order $\bar{\mathbf{I}}^{(3-1)}$ (dash-dotted line).

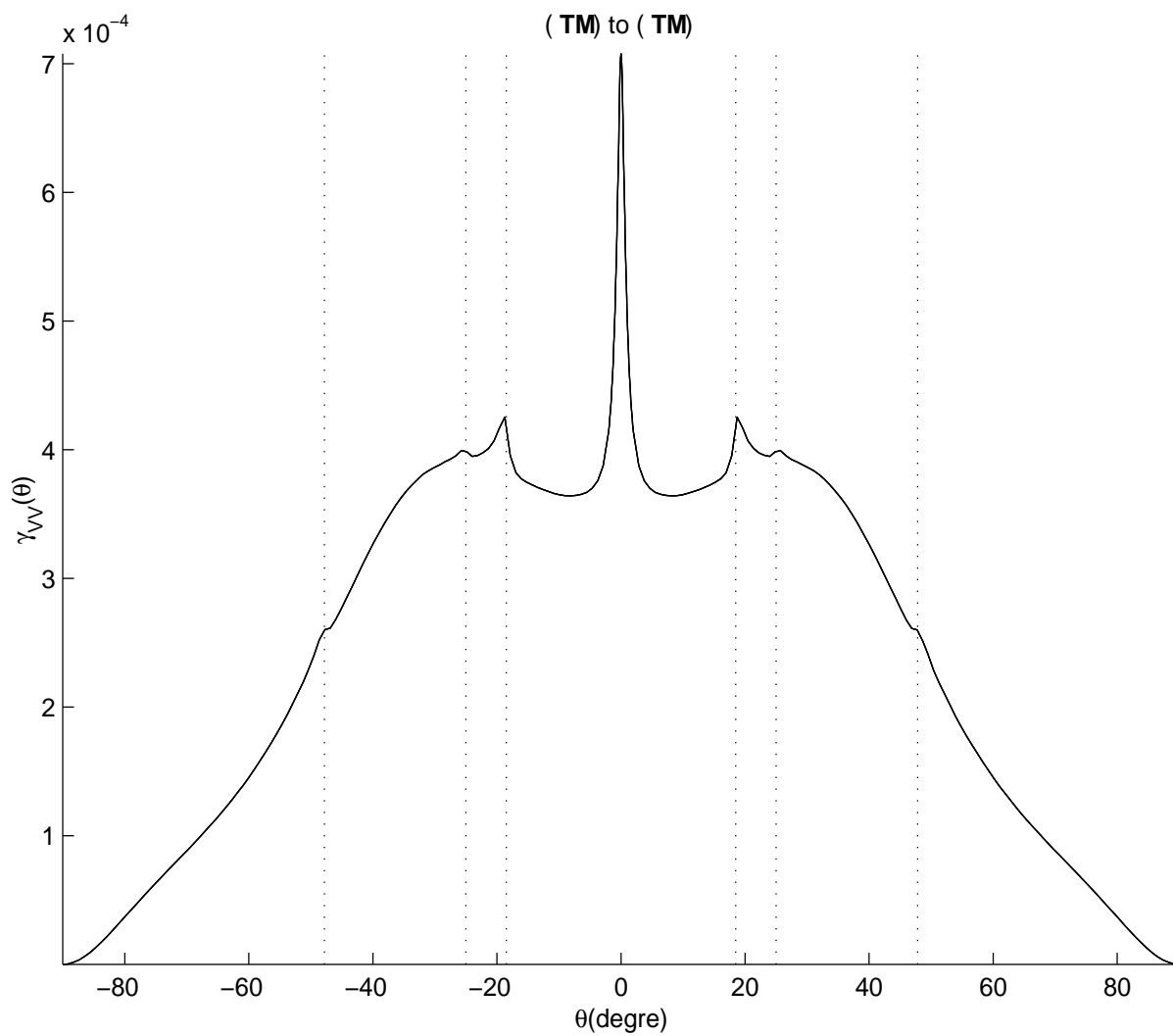


FIG. 15: Details of the second order (*TM*) to (*TM*) contribution to the scattering shown in Fig. 14, dotted lines mark the peaks angle position.

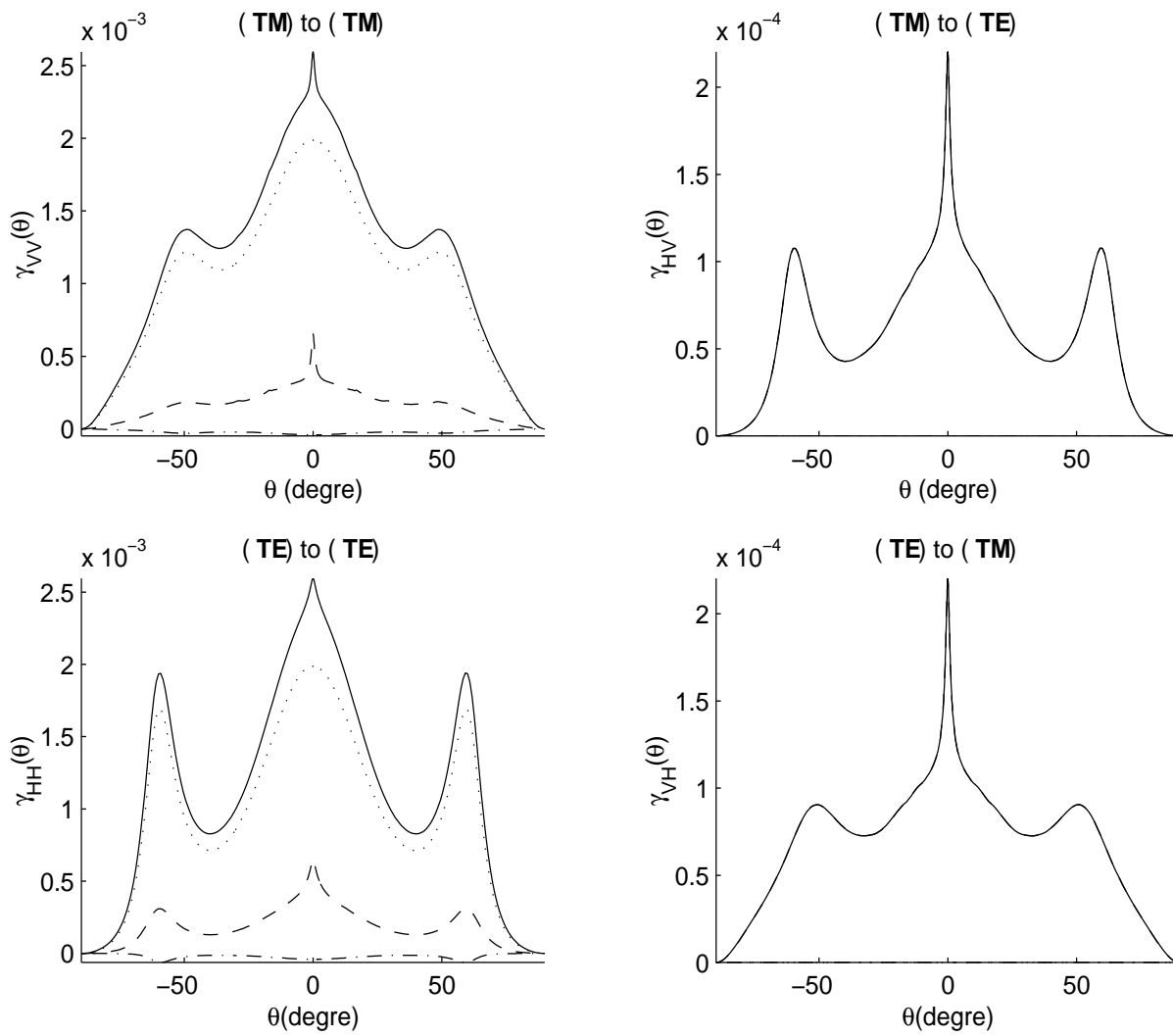


FIG. 16: Effect of the slab thickness, $H = 1000\text{nm}$, on the configuration shown in Fig. 14.

